STUDIA
UNIVERSITATIS BABEŞ-BOLYAI

PHYSICA

2

1991

CLUJ-NAPOCA

Anul XXXVI 1991

S T U D I A

UNIVERSITATIS BABEŞ-BOLYAI

PHYSICA

2

R e d a c ţ i a : 3400 CLUJ-NAPOCA str. M. Kogălniceanu nr.1 ► Telefon: 116101

S U M A R - C O N T E N T S - S O M M A I R E

M. COLDEA, A. GIURGIU, T. PETRISOR, The effect of Ti substitution for Cu on the superconducting properties of $NdBa_2Cu_3O_{7-y}$ 3

V. POP, E. BURZO, Physical properties of Zr - substituted $YBa_2Cu_3O_{7-\delta}$ - superconducting compounds 9

A. V. POP, Al. NICULA, L.V. GIURGIU, Al. DARABONT, The treatment in oxygen atmosphere and EPR absorbtion in $(Y_{1-x}\ Gd_x)$-Ba-Cu-O system 23

V.A. BUDYANU, I.A. DAMASKIN, S.A. FEDISEEV, S.L. PYSHKIN, VAL.P. ZENCHENKO, VIT.P. ZENCHENKO, Spectroscopy of laser produced plasma from $YBa_2Cu_3O_{7-x}$ - ceramics 29

L.MIU, "Peak effect" in high-T_c superconducting ceramics 39

L. MACARIE, L.VASILIU-DOLOC, F.BUZATU, M. APOSTOL, On the superconducting critical temperature of $La_{2-x}Ba_xCuO_4$ 45

T. PETRISOR, L. CIONTEA, A. GIURGIU, DC - Magnetron Sputtering Gun for HT_cS films deposition 59

STUDIA UNIV. BABEŞ-BOLYAI, PHYSICA, XXXVI, 2, 1991

THE EFFECT OF Ti SUBSTITUTION FOR Cu ON THE SUPERCONDUCTING PROPERTIES OF $NdBa_2Cu_3O_{7-y}$.

Marin COLDEA[1], Alin GIURGIU[2] and Traian PETRIŞOR[2]

ABSTRACT. The electrical resistance of $NdBa_2Cu_{3-x}Ti_xO_{7-y}$ (x=0; 0.05 and 0.20) was measured in the temperature range 50-280K. The Ti ions remarkably affect superconductivity and depress the critical temperature T_c. The orthorhombic-to-tetragonal phase transition is discussed in terms of a large instability to oxygen variation.

1. INTRODUCTION. Up to date there is a large number of experimental papers dealing with the investigations of the substitution effects in high-T_c superconductive oxides. Earlier studies on $YBa_2Cu_{3-x}M_xO_{7-y}$ compounds, in which Cu atoms are partially replaced by magnetic or nonmagnetic 3d metal M, revealed that the mechanism for high-temperature superconductivity must show a sensitivity to local structural order[1,2]. This view is consistent with the short coherence length in these materials[3]. In addition to the intrinsec impurity effects, the observed reduction in T_c by doping may partly be attributed to various other factors, especially to those associated with oxygen content. The metallic-superconducting phase in the undoped compounds RBa_2Cu_3O7-y is unstable to the loss of oxygen and becomes systematically more unstable as the ion size of the rare earth element R increases[4]. So, the transition temperature T_c approaches OK in $NdBa_2Cu_3O_{7-y}$ for y=0.42 and in YBa_2Cu_3O7-y for y=0.64[4].

The aim of this paper is to study the effect of Ti substitution for Cu on the superconducting properties of $NdBa_2Cu_3O_{7-y}$ which has a large instability to oxygen variation.

2. EXPERIMENTAL. The samples studied in this work were prepared by a solid state reaction in air. Powders of Nd_2O_3, $BaCO_3$, CuO and TiO_2, all with a purity of 99.99%, were mixed,

---

[1] *Faculty of Physics, University of Cluj-Napoca, Str. M Kogălniceanu nr.1, 3400 Cluj-Napoca, Romania.*

[2] *Polytechnic University, Physics Department, Str.C.Daicoviciu nr.15, 3400 Cluj-Napoca, Romania.*

pressed into pellets and heated at 950°C for 24 hours. The reacted pellets were reground, pressed again into pellets and sintered at 950°C for 12 hours at oxygen pressure of 1.2 bar. The electrical resistance of all samples was measured by the d. c. four-probe method. A current of 1mA was used. The temperature down to 50K was attained by vacuum evaporation of liquid nitrogen.

3. RESULTS AND DISCUSSION. Figure 1 shows the temperature dependence of the electrical resistance for $NdBa_2Cu_{3-x}Ti_xO_{7-y}$ with x=0; 0.05 and 0.20.

On the same figure is also plotted the dependence R(T) for $YBa_2Cu_3O_{7-y}$ has a narrow phase transition (ΔT_c<4K and T_c=93K) and exhibits metallic behaviour above the transition. These data

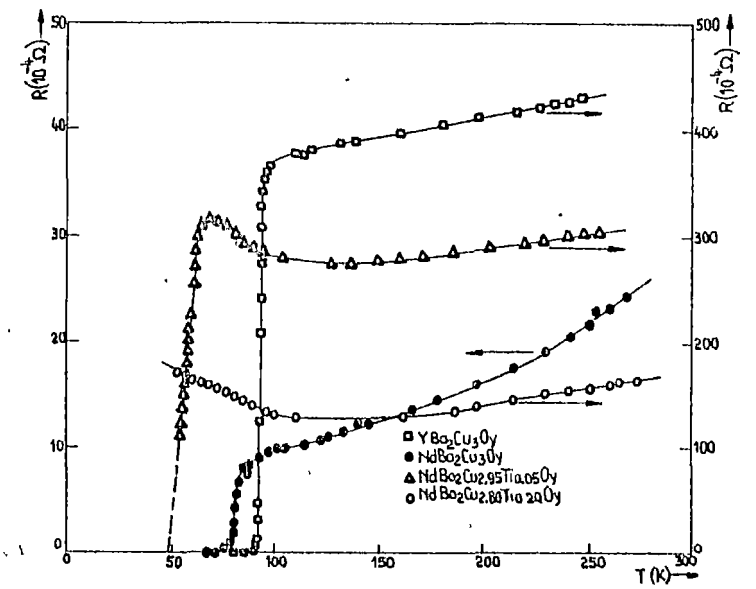

Figure 1. Resistance versus temperature in $YBa_2Cu_{3-x}Ti_xO_{7-y}$ for several concentrations of Ti

confirme the good quality of the sample and that she was sufficient oxygenated. This is not the same for $NdBa_2Cu_3O_{7-y}$, i.e. in the normal state the dependence R(T) is not linear and $\Delta T_c \approx 10K$ with $T_c=80K$. The difference in the superconducting properties of the two compounds shows that the sample $NdBa_2Cu_3O_{7-y}$ was not fully oxygenated. This may be caused by the large difference in the ionic radii of Y and Nd. Effective ionic radii in 8-fold coordination, as given by Shannon[5] are Y(0.99A) and Nd(1.10A). However, fully oxygenated samples of $NdBa_2Cu_3O_{7-y}$ with T_c above 90K were obtained by Neumeier et al[6]. and by Veal et al[4]. for high values of the sintering times in oxygen atmosphere. The differences with our results are probably connected with the lower sintering time and the more rapid cooling in oxygen atmosphere. In order to explain the nonlinear increase of the resistance with temperature in the normal state for $NdBa_2Cu_3O_{7-y}$, we assume that the system of the charge carriers is described by two energy state W_1 and W_2. In this case the total conductivity is given by

$$\sigma = \sigma_1 P_2(T) + \sigma_2 P_2(T) \qquad (1)$$

where P_1 and P_2 are the tunneling probabilities for the charge carriers. Taking into account the relations between these probabiliyies one obtains

$$\sigma = \sigma_1 - (\sigma_1 - \sigma_2) e^{-\Delta W/kT} \qquad (2)$$

for the case $W_1<W_2$ and $\sigma_2<\sigma_1$. From this formula results for temperature dependence of the resistivity the relation

$$\ln(\rho - \rho_1) = \ln\rho_1(1 - \rho_1/\rho_2) - \Delta W/kT \qquad (3)$$

and a similar expression for R(T). As one can see from Figure 2, the experimental results are well described by equation (3) with $R_1=9.6\times10^{-4}\Omega$ as fit parameter.

The Ti substitution for Cu in $NdBa_2Cu_{3-x}Ti_xO_{7-y}$ affects very strong the superconductivity and depress the critical temperature T_c(Fig.1). For only 1.66% Ti(x=0.05), the critical temperature decreases to 50K. The samples with Ti show semiconductor behaviour with a negative temperature derivative of resistance, $dR/dT<0$ towards lower temperatures. The values of the resistance in doped samples are with one order of magnitude larger than in

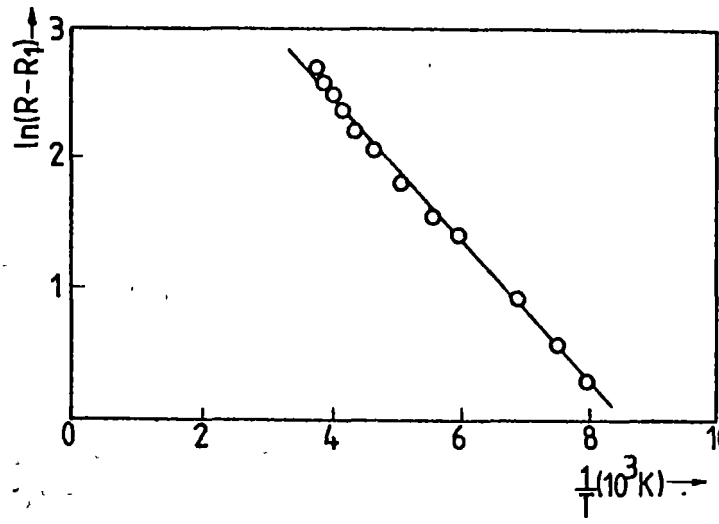

Figure 2. The logarithm of the resistance versus reciprocal temperature for $NdBa_2Cu_3O_{7-y}$.

undoped samples. On the other hand, comparing the values of the resistances for the doped samples one may conclude that the slope dR/dT in the low temperature region for x=0.20 is much larger than that for x-0.05. This means that the semiconductor character of the sample with x=0.20 is much more pronounced than for x=0.05 and probably the compound $NdBa_2Cu_{2.80}Ti_{0.20}O_{7-y}$ does not show superconductivity even at very low temperatures. Earlier studies of Maeno et al[2]. on $YBa_2Cu_{2.90}Ti_{0.10}O_{7-y}$ pointed out that Ti ions have no influence on the superconducting properties of the parent compound. The above authors concluded that Ti is almost entirely excluded from the parent structure and are not introduced into the Cu sites. Contrarily, the strong effect of Ti substitution for Cu on the superconductivity of $NdBa_2Cu_3O_{7-y}$ demonstrates that Ti replace Cu atoms in the parent structure. An important challenge in the Cu substitution experiments is to determine exactly which Cu site the dopant occupies. A large electronic disturbance introduced by Ti ions in the Cu 1 site may explain the destabilization of the ordering of oxygen in the

parent orthorhombic structure, inducing the transition to the tetragonal structure.

R E F E R E N C E S

1. Tarascon J.M., Barboux P., Micell P.F., Greene L.H.and Hull G.W., **Phys.Rev. B37**, 7458 (1988)
2. Maeno Y. and Fuzita T., **Physica C 153-155**, 1105 (1988)
3. Bednorz J.G.and Muller K.A., **Rev.Mod.Phys. 60**, 585 (1988)
4. Veal B.V., Paulikas A.P., Downey J.W., Claus H., Jensen M., Vandervoort K., Tomlins G., Shi H.and Morss L., **Physica C 162-164**, 97 (1989)
5. Shannon R.D., **Acta Crystallogr. A32**, 751 (1976)
6. Neumeier J.J., Dalichaouch Y., Hake R.R., Lee B.W., Maple M.B., Torıkachvili M.S.and Yang K.M., **Physica C 152**, 293 (1988)

STUDIA UNIV. "BABEŞ-BOLYAI", PHYSICA, XXXVI, 2, 1991

PHYSICAL PROPERTIES OF Zr-SUBSTITUTED $YBa_2Cu_3O_{7-\delta}$ SUPERCONDUCTING COMPOUNDS

Viorel POP[1] and Emil BURZO[2]

ABSTRACT. The results of X-rays, electric resistivities and magnetic measurements performed on $Y_{1-x}Zr_xBa_2Cu_3O_{7-\delta}$ and $Y_{1-2x}Zr_xEu_xBa_2Cu_3O_{7-\delta}$ superconducting compounds, in the temperature range 4.2-500K and fields up to 50 kOe are reported. The presence of zirconium leads to a decrease of the superconducting transitions temperature, T_c. Below the transition temperature, the hysteresis curves are narrowed as Zr content increases. A time dependence of the magnetizations of logarithmic form is also evidenced. Above the transition temperatures, $Y_{1-x}Zr_xBa_2Cu_3O_{7-\delta}$ samples show a Pauli-type paramagnetism while $Y_{1-2x}Zr_xEu_xBa_2Cu_3O_{7-\delta}$ compounds have temperature dependent susceptibilities. The effective europium moment is ~ 3.40 μ_B suggesting that it is in (+3) valence state.

1. INTRODUCTION. The effect of ZrO_2 addition on the resistive behaviour of $YBa_2Cu_3O_{7-\delta}$ -base compounds has been previously reported [1]. The partial replacement of Y and both Y and Ba by Zr results in the formation of multiphase superconducting system. The substitution of cooper by zirconium leads to a single superconducting phase.

In this paper we report the physical properties of $YBa_2Cu_3O_{7-\delta}$ superconducting compounds, where yttrium has been gradually replaced by Zr or both Zr and Eu. The evolution of superconducting transition temperatures, hysteresis curves, critical fields and magnetic behaviour above transition temperatures were investigated. Yttrium is in (+3) valence state, while zirconium has a (+4) valence. Europium may be both in (+2) and (+3) valence states. Thus, is also of interest to analyse to what extent, the presence of zirconium will induce another

[1] *Faculty of Physics, University of Cluj-Napoca, Str. M.Kogălniceanu nr.1, 3400 Cluj-Napoca, Romania.*

[2] *Institute of Isotopic and Molecular Technology, 3400 Cluj-Napoca, P.O.Box 700, Romania*

valence state than (+3) characteristic for europium in $EuBa_2Cu_3O_{7-\delta}$ compound.

2. EXPERIMENTAL. The samples were prepared by solid state reaction. The mixture of Y_2O_3, EuO, CuO, ZrO_2 and barium carbonate, in required proportions, were homogeneized, finely grinded and calcinated. The calcination has been made at temperatures between 920 and 950°C, in oxygen atmosphere. After calcination the sample structure was analysed by X-rays. The formation of perovskite-type structure is evidenced in all cases. The calcinated samples were finely grinded and then compacted at a pressure of 3 t/cm^2. The calcination and sintering temperatures, required to have highest superconducting transition temperatures, decrease when Y is gradually replaced by (Eu+Zr). The sintering has been performed in the temperature range (930-960)°C, in oxygen atmosphere. The samples were then slowly cooled.

The densities of the sintered materials were (88-95)% from theoretical density. After keeping 8 mounths in air, no degradation of sample properties was evidenced.

The X-ray analysis, in all cases, show the presence of orthorombic-type structure. In addition, small quantities of ZrO_2 were evidenced for samples having an initial content greater than x=0.2. The free ZrO_2 content is estimated at 20% from the initial content both after calcination and sintering processes. Previously [1] no quantitative information on the structure of zirconium substituted $YB_2Cu_3O_{7-\delta}$ were reported.

Electrical resistivity measurements were made by using a standard four probe technique, in the temperature range 77-300K.

The magnetic studies were performed with an "Oxford Instruments" equipment, in the temperature range 4.2-300 K and external fields up to 50 kOe. For higher temperatures than 300 K, the magnetic susceptibilities were determined by using a Faraday-type balance.

3. EXPERIMENTAL RESULTS. The temperature dependences of the electrical resistivities for some representative compounds are plotted in figure 1. The ZrO_2 addition decreases somewhat the superconducting transition temperatures, T_c, but still remain higher than 84 K, for x=0.2. For the $Y_{0.6}Zr_{0.2}Eu_{0.2}Ba_2Cu_3O_{7-\delta}$ sample, the T_c value increase up to 90 K.

The evolution with temperature of the hysteresis curves obtained for $Y_{0.8}Zr_{0.1}Eu_{0.1}Ba_2Cu_3O_{7-\delta}$ compound is shown in figure 2. As the temperature increases the hysteresis curves become narrower. For the same ZrO_2 content the hysteresis curves are more constricted in samples without europium (figure 3).

Magnetization hysteresis loops are traditionally used to estimate H_{c1} values. The field dependence of the magnetization, at 4.2 K, in low external fields are plotted in figures 4 and 5, for $Y_{0.3}Zr_{0.7}Ba_2Cu_3O_{7-\delta}$. The H_{c1} values in figure 4 were identified as the field where M(H) curve deviates from linearity. For the above sample the critical field is H_{c1}= 260 Oe. The magnetization curves appering in different ranges of fields sugggest that two kinds of "materials" are coexisting in the sample:

superconducting grains and the boundary materials between the grains. Because of tunneling or proximity effect the Cooper pairs can pass through these regions. It can be called weak link granular superconductivity [2]. Up to H_{c1}= 260 Oe, the contribution of grains to the total magnetization is a reversible strait line. The hysteretic contribution is

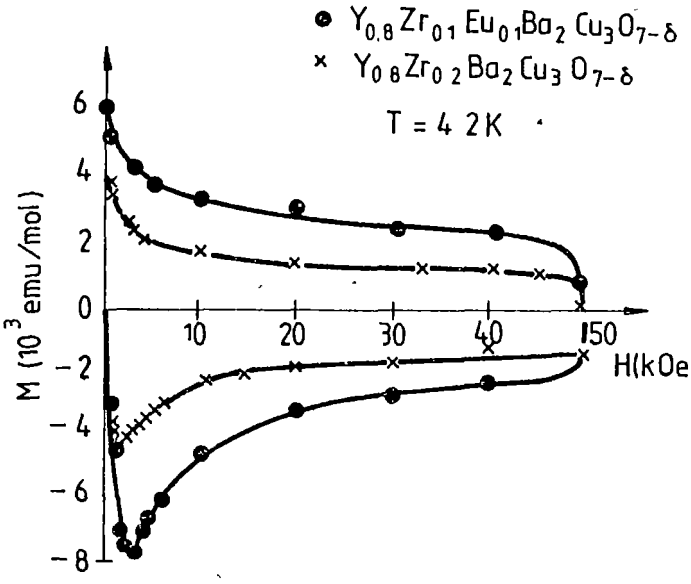

Figure 3. The hysteresis curves for the studied samples at 4.2 K.

due to weak link superconductivity. When $H<H^{W}_{c1}$ (H^{W}_{c1}≈41 Oe), there is a shielding current around the surface of the whole

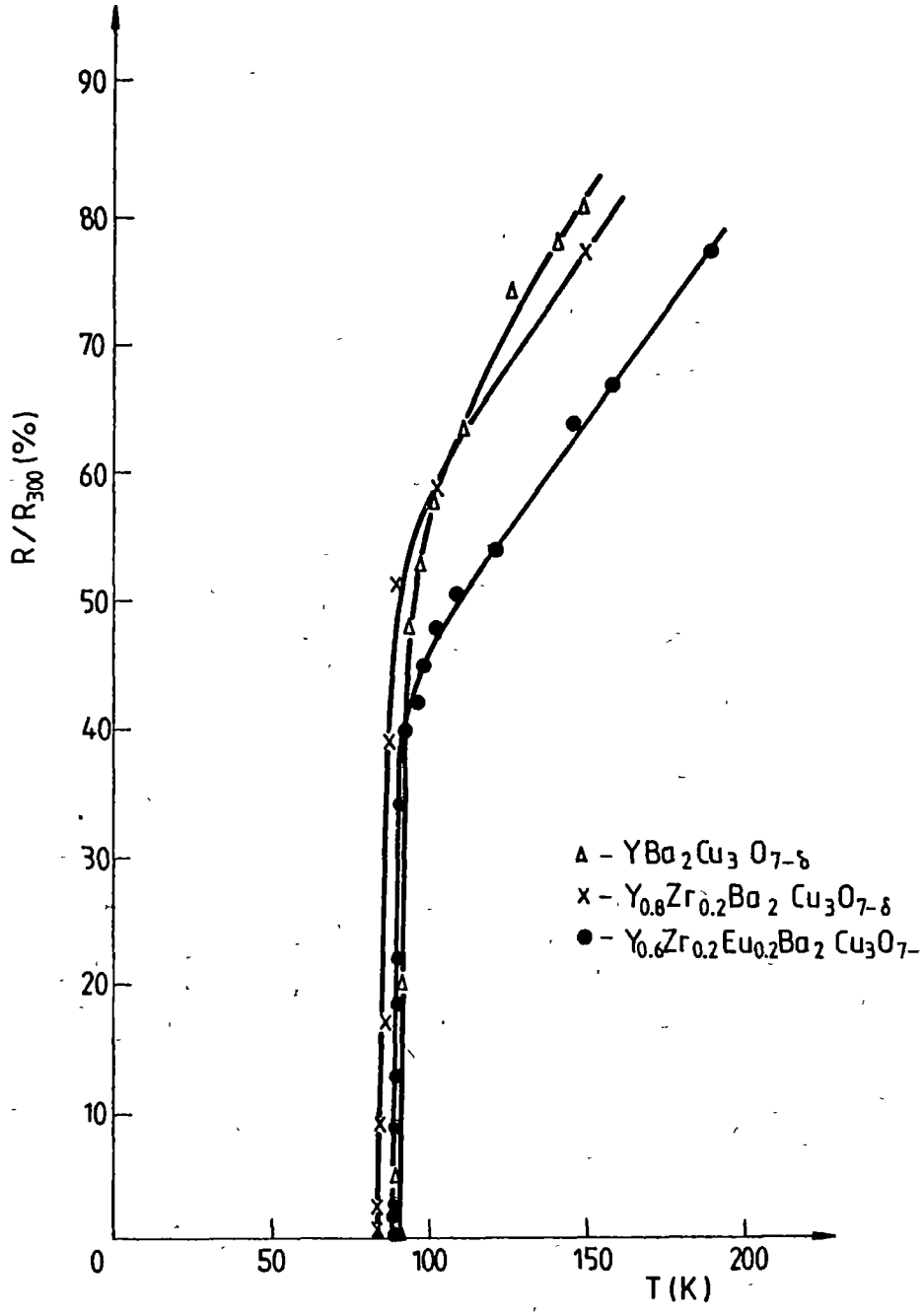

Figure 1. Temperature dependences of the electrical resistivities for some $YBa_2Cu_3O_{7-\delta}$ based compounds.

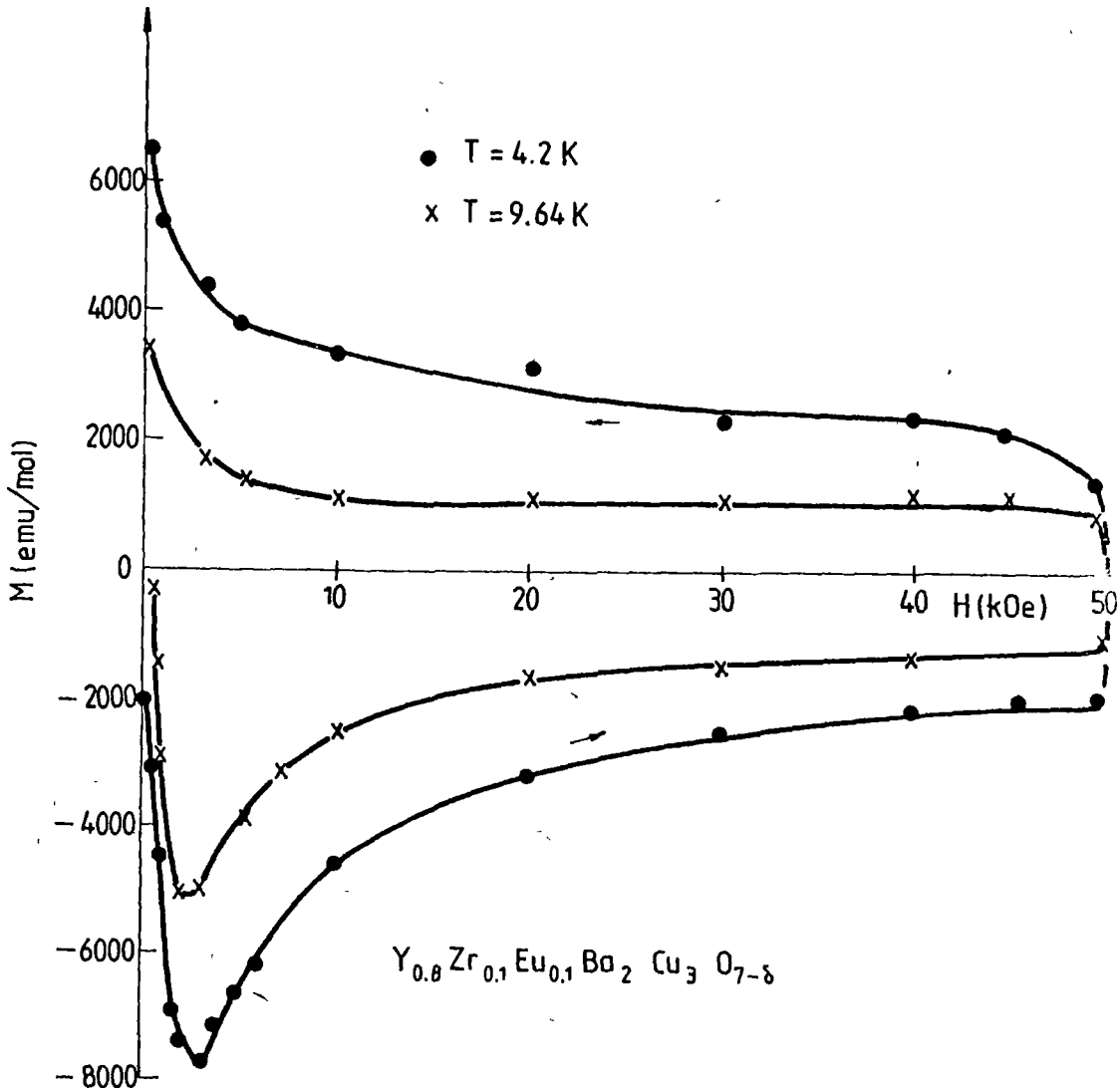

Figure 2. Magnetic hysteresis loops for $Y_{0.8}Zr_{0.1}Eu_{0.1}Ba_2Cu_3O_{7-\delta}$ at 4.2 and 9.64 K.

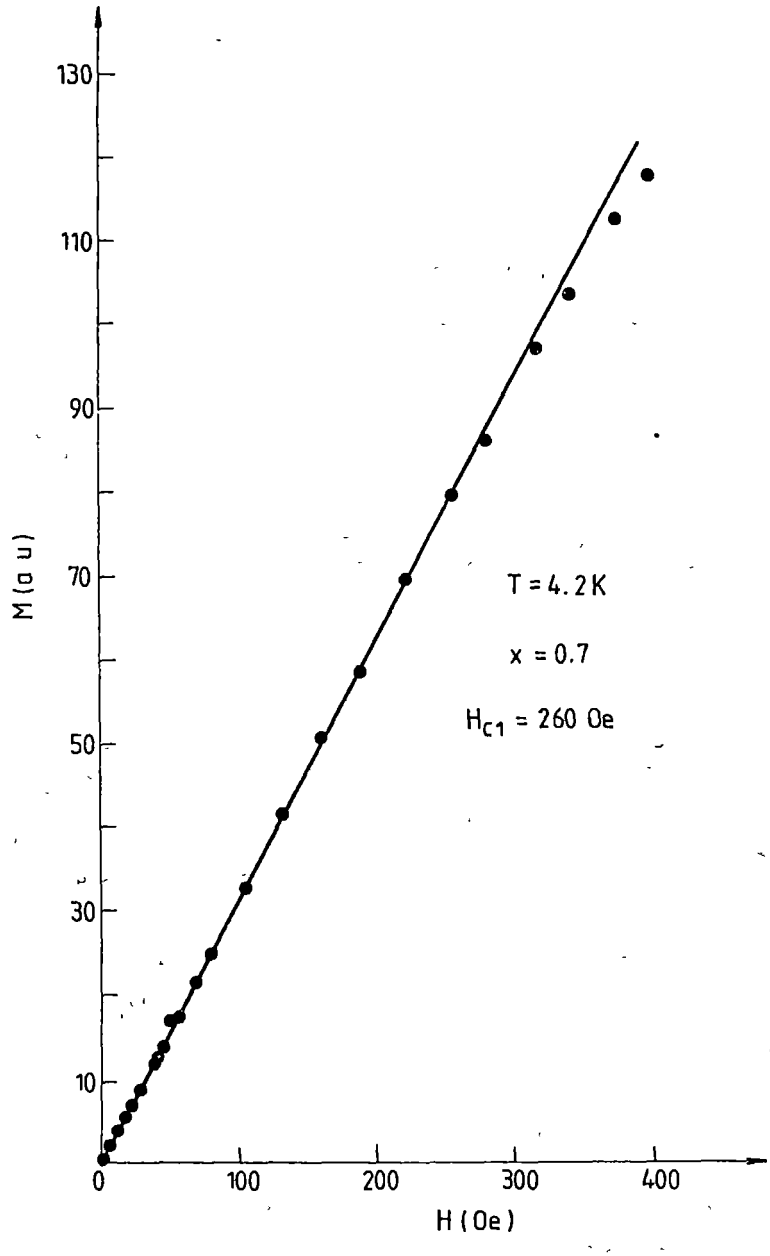

Figure 4. Field dependence of magnetization at 4.2 K for $Y_{0.7}Zr_{0.3}Ba_2Cu_3O_{7-\delta}$, in low fields.

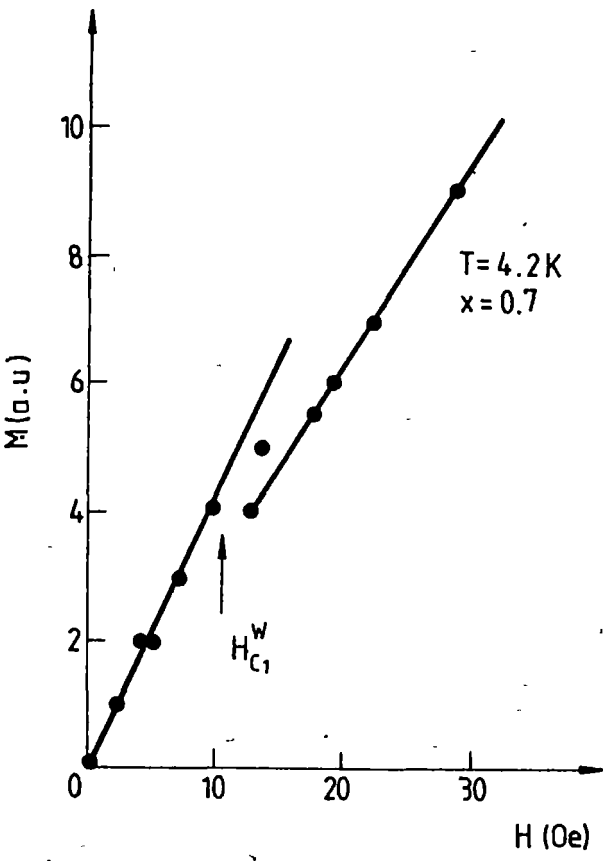

Figure 5. The field dependence of the magnetization, at 4.2 K, in low external fields, H<40 Oe.

sample which is in the Meissner state. The magnetic penetration depth is the London penetration depth and the shielding current results in a slope which is greater than obtained at higher fields (figure 5). When $H = H^W_{c1}$, the magnetic flux begins to penetrate into boundary materials between the grains. Because of pinning, magnetic hysteresis appears, and the weak coupling supercurrent around the whole sample exists inside

all the magnetic penetration regions. The H^W_{c1} is called lower critical field of the weak link granular superconductor. At a field H^W_p~45 Oe, the field of full penetration for weak link superconductor, the flux penetrates into the whole sample (but not inside the grains). The field H_{c1} is the low critical field of the superconducting grains. It is to be mentioned that the field H^W_p is identified by a small change of slope in figure 4.

The time dependences of the magnetizations at various fields and temperatures were also analysed. Some data are plotted in figures 6 and 7. After an initial period, the magnetization shows a time dependence of the logarithmic form

$$M(T) = M(0) + S \ln (t/t_0) \quad (1)$$

The classical flux creep model will be used to analyse these data [3-7]. The model considers a type II superconductor with a conventional Abrikosov` vortex of flux line lattice. Inhomogeneities in the material cause pinning of these vortices in potential valley of height U_o. Such pinning prevents motion of vortices in the presence of current, thus controlling the critical current density, j_c. The thermal activation of flux lines over the potential barrier induces magnetic relaxation and reduction of critical current

$$j_c = j_{co}[1 - (k_B T/U_o) \ln(t/t_o)] \quad (2)$$

where j_{co} is the critical current in the absence of thermal fluctuations.

The magnetization relaxation of a cylinder of radius r is derived by substituting (2) into the original Bean's equation [7]

$$dM/d(\ln t) = S = j_c j/3c \; k_B T/U_o \quad (3)$$

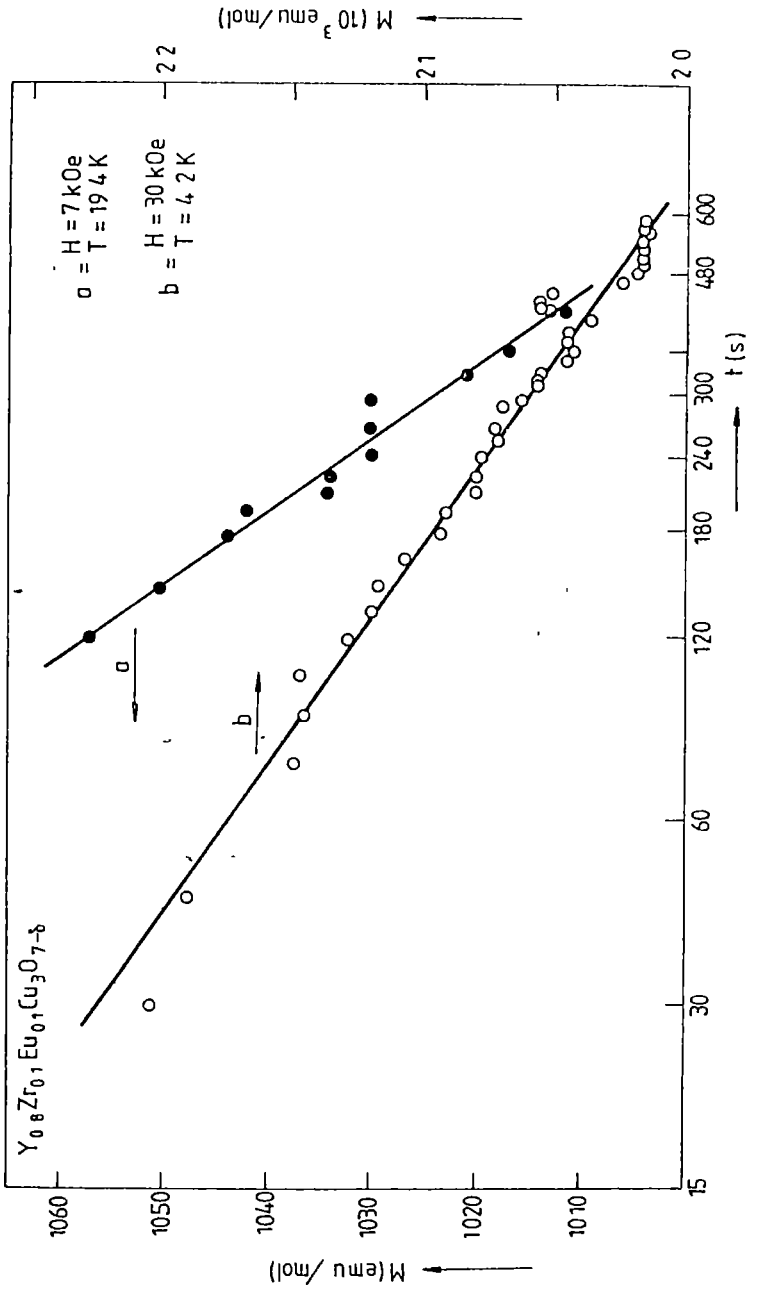

Figure 6. Time dependence of magnetization for $Y_{0.8}Zr_{0.1}Eu_{0.1}Ba_2Cu_3O_{7-\delta}$ at 4.2 K various external fields.

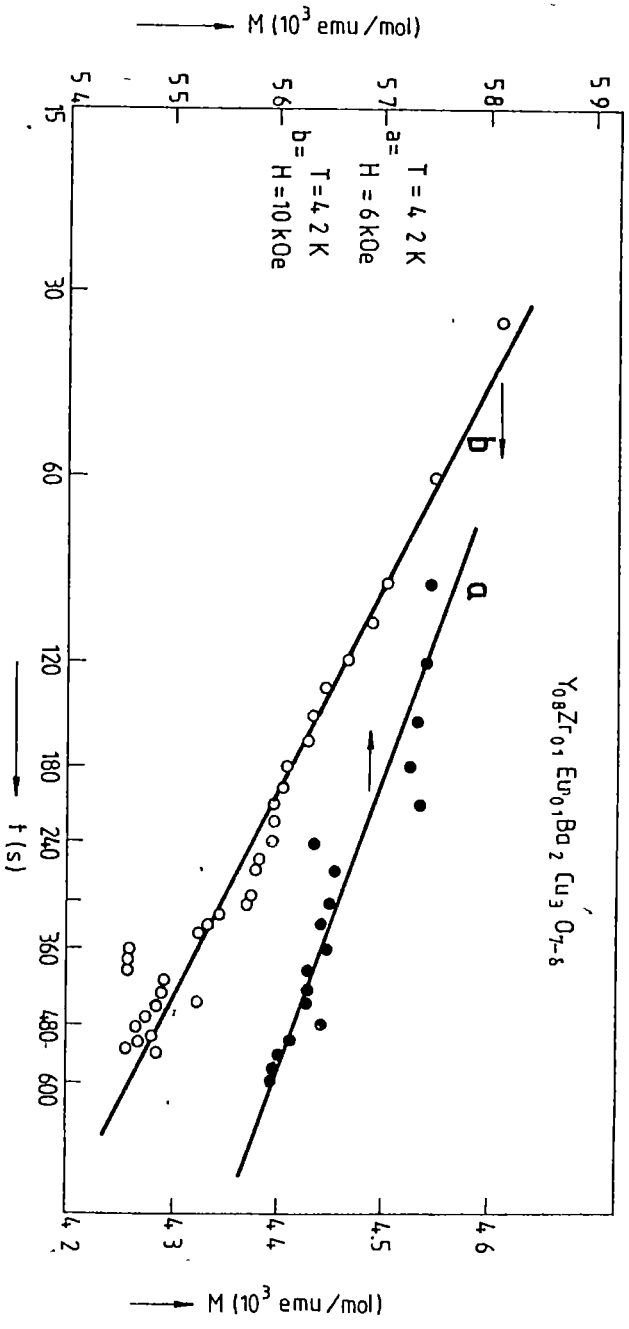

Figure 7. The dependence of the magnetization for $Y_{0.8}Zr_{0.1}Eu_{0.1}Ba_2Cu_3O_{7-\delta}$ at various temperatures and fields.

where c is the light speed. In the above relation a correction term, due to the field dependence of U_o and j_c was neglected. Really the S values may be changed by the field by~30% with a maximum at H~18 kOe [8]. From the temperature dependences of j_c values we estimated U_o~0.1 eV. A detailed discussion on the composition dependence of the energy for flux pinning has published [9].

The $Y_{1-x}Zr_xBa_2Cu_3O_{7-\delta}$ samples show a Pauli-type paramagnetism. The determined values of susceptibilities are $0.48x10^{-6}$ emu/g for x = 0.1 and $0.87x10^{-6}$ emu/g for x = 0.2.

In case of $Y_{1-2x}Zr_xEu_xBa_2Cu_3O_{7-\delta}$ compounds, in addition to a Pauli paramagnetic contribution χ_o, a temperature dependent term is also present (figure 8). The susceptibilities may be described by the relation

$$\chi = \chi_o + C(T - \theta)^{-1} \qquad (4)$$

By fitting the experimental data, according to (4), the χ_o, C and θ parameters were determined. The paramagnetic Curie temperatures, θ are negative and smaller than 5 K, in absolute magnitude. The temperature independent contribution, χ_o, are close the susceptibilities determined in corresponding $Y_{1-x}Zr_xBa_2Cu_3O_{7-\delta}$ samples. From the Curie constants, C, the effective europium moments M_{eff} were determined. The M_{eff} values are around 3.40 μ_B, suggesting that the europium ions are in (+3) valence state. Thus, the presence of Zr^{4+} ions in lattice seems to not change the valence state of europium.

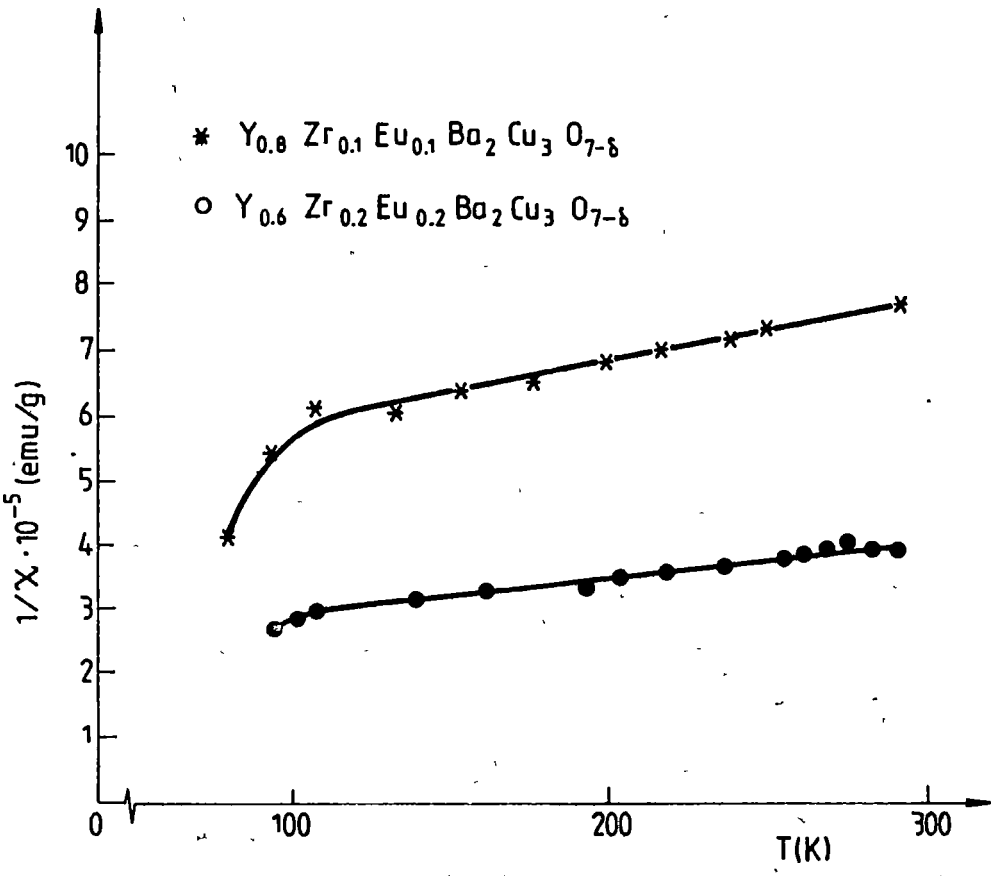

Figure 8. Thermal variations of reciprocal susceptibilities for $Y_{0.8}Zr_{0.1}Eu_{0.1}Ba_2Cu_3O_{7-\delta}$ and $Y_{0.6}Zr_{0.2}Eu_{0.2}O_{7-\delta}$ at $T>T_c$.

4. CONCLUSIONS. The presence of zirconium decrease somewhat the superconducting transition temeprature of $Y_{1-x}Zr_xBa_2Cu_{7-\delta}$ based compounds. This decrease is partially recovered when yttrium is substituted by both zirconium and europium. In addition to the familiar first critical field, H_{c1}, two more characteristic fields were identified at low external fields. Such a complex magnetic behaviour is a direct consequence of a

highly inhomogeneous distribution of critical current densities within the samples. The critical currents depend on the local metallurgical defects, the most common being the barriers between the grains (weak superconductor links) and the surface of grains.

The magnetizations show a time dependence of the logarithmic form. The data may be well decribed in the classical flux creep model. The energies for flux pinning are of the order of 0.1 eV. The magnetic creep constants are dependent on the temperature and field, with a maximum located at H≈18 kOe. At $T>T_c$ the $Y_{1-x}Zr_xBa_2Cu_3O_{7-\delta}$ compounds are Pauli paramagnets. The presence of europium as in $Y_{1-2x}Eu_xZr_xBa_2Cu_3O_{7-\delta}$ leads to temperature dependent contributions to susceptibilities. From the effective moments it is concluded that europium is in (+3) valence state.

REFERENCES

1. Yayaram B., Agarawal S.K., Nagtal K.C., Gupta A., Narlikan A.V., **Mat. Res. Bull. 28**, 701 (1988)
2. Yu Y., **Mat. Sci. Forum 62-64**, 137 (1990)
3. Anderson P.W., **Phys. Rev. Lett. 9**, 309 (1962)
4. Anderson P.W., Kim Y.B., **Rev. Mod. Phys. 36**, 89 (1964)
5. Beasley M.R., Labusch R., Weeb W.E., **Phys. Rev. 181**, 682 (1969)
6. Campbell A.M., Evetts J.E., **Adv. Phys. 21**, 199 (1972)
7. Bean C.P., **Phys. Rev. Lett. 8**, 250 (1962); **Rev. Mod. Phys.36**, 31 (1964).
8. Pop V., Burzo E., **Mater. Sci. Forum 62-64**, 205 (1990)
9. Burzo E., Pop V., **J. Mat. Sci.27**, 5253 (1992)

STUDIA UNIV. BABEŞ-BOLYAI, PHYSICA, XXXVI, 2, 1991

THE TREATMENT IN OXYGEN ATMOSPHERE AND EPR ABSORPTION IN $(Y_{1-x}Gd_x)$-Ba-Cu-O SYSTEM

A.V.POP[1], AL.NICULA[1], L.V.GIURGIU[2] and AL.DARABONT[2]

ABSTRACT. EPR measurements were performed in the $Y_{1-x}Gd_xBa_2Cu_3O_{7-\delta}$ superconducting system prepared in oxygen atmosphere. The change of EPR linewidth ΔB_1 for Gd^{3+} versus x evidenced the decrease of Gd^{3+}-Cu^{2+} interactions in the oxygenated samples by comparison with samples treated in air. The qualitative analyse of dipolar and exchange interactions were performed.

1.INTRODUCTION. Superconductivity above 90K has been found in the series of rare earth ion such as Gd and significant EPR signals due to Gd^{3+} ions were observed [1-5]. One of the striking features of $RBa_2Cu_3O_y$ type high-T_c superconductors is that this high-T_c superconductivity is not destroyed by the localized moments of the rare earth (R) ions. In order to measure the magnetic and crystal field interactions using the EPR of localized moments, the partial substitution of rare-earth element such as Gd for Y in Y-Ba-Cu-O system has been used [6-10].

Here we present a report of our EPR measurements at 9,25 GHz and room temperature on $Y_{1-x}Gd_xBa_2Cu_3O_{7-\delta}$ sample $(0.01 \leq x \leq 1)$ treated in oxygen atmosphere. The observed spectra in samples treated in air [7,10] and oxygen indicate the overlapping over the characteristic Gd^{3+} line of a signal typically for Cu^{2+} resonance. An analysis of Gd^{3+} linewidth as a function of x is presented.

---

[1] *Faculty of Physics, University of Cluj-Napoca, Str.M.Kogălniceanu nr.1, 3400 Cluj-Napoca, Romania*

[2] *Institute of Isotopic and Molecular Technology, 3400 Cluj-Napoca, P.O.Box 700, Romania.*

2. EXPERIMENTAL. The samples were prepared from mixtures of Gd_2O_3, Y_2O_3, $BaCO_3$ and CuO powders by the solid phase reaction method [10]. The pellets were sintered in flowing air (samples # 1) or in oxygen atmosphere (samples # 2) at 80°C and cooled down to room temperature at a rate of 10°C/min.

The presence of a superconducting phase with T_c>77K was established by testing the Meissner-Ochsenfeld effect under liquid nitrogen temperature (LNT). The EPR measurements at x-band were carried out by means of a Radiopan SE-X/2543 with 100 kHz field modulation at room temperature. The samples prepared for EPR measurements were finely crushed and mixed with silicon fett Merck. The analysis of the EPR lineshape for samples at RT indicates the overlapping over the Gd^{3+} line of a signal centred at g=2.060 ± 0.002. The EPR spectra of samples # 2 show a reduction of the intensity of the Cu^{2+} line compared with the corresponding signal for the same mass of samples # 1. We belive that this result strongly indicates that the decrease of the number of Cu^{2+} ion in the chains is produced by the oxygenation of the sample. In order to obtain some informations concerning the magnetic interaction in our samples we have to discuss the linewidths. In Fig.1 we plotted the peak-to peak linewidth ΔB_1 for Gd^{3+} ions in samples # 1 and # 2 as a function of x.
The lower ΔB_1 values for samples # 2 can be explained by the decrease of the Gd^{3+}-Cu^{2+} magnetic interactions. The fact that the Cu^{2+} signal persist in samples # 2 is probable caused by the impurity insulating phases $(Y_{1-x}Gd_x)_2BaCuO_5$ [3,11].
The linewidth analysis of dipolar contribution for the

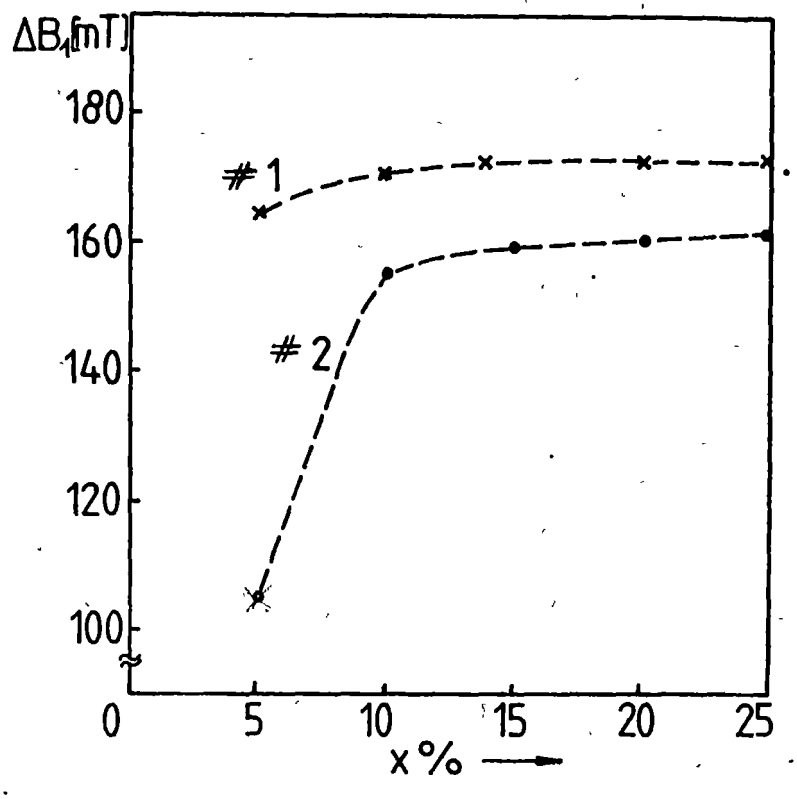

Figure 1. The dependence of Gd^{3+} linewidth as a function of x is samples # 1 and # 2.

superconducting samples # 1 and # 2 were performing assuming: $\Delta B_1 \sim x$, for a Lorentzian lineshape and $\Delta B_1 \sim \sqrt{x}$, for a Gaussina lineshape.

A comparison of these theoretical dependences of B, versus x with the experimental results for Gd^{3+} linewidth, show the presence a supplimentary broadening of the EPR linewidth as in Fig.2.

This fact may be an indication of the presence of

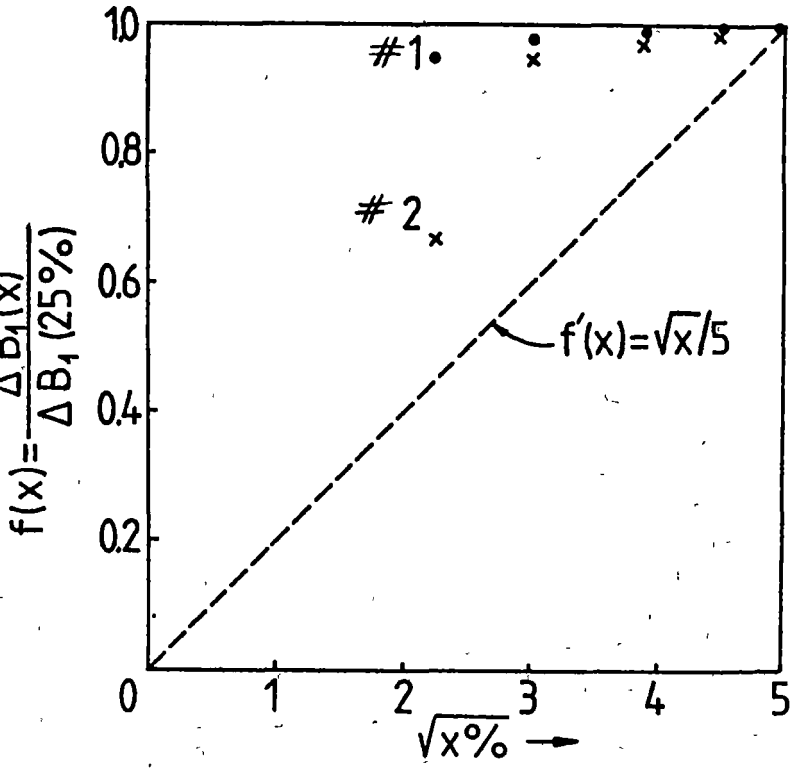

Figure 2. The linewidth analysis of dipolar contribution for the samples # 1 and # 2. The dotted line represent the teoretical dependence $\Delta B_1 \sim \sqrt{x}$ for a Gaussian lineshape.

anisotropic exchange interaction as a source of the line broadening.The fact that we observed the superimposed Gd^{3+} and Cu^{2+} resonances suggests that the Gd^{3+}-Cu^{2+} magnetic interactions are quite weak.

REFERENCES

1. Schwartz R.N., Pastor A.C., Pastor R.C., Kirby K.W. and Rytz D., **Phys.** Rev. B 36, 8858 (1987).
2. Mehran F., Barnes S.E., Tsuci C.C. and Mc Guire T.R.,**Phys. Rev. B 36,** (1987).
3. Mehran F., Barnes S.E., Tsuci C.C. and Mc Guire T.R.,**Solid State Commun.** 67, 55 (1988).
4. Kikuchi H., Ajiro Y., Kosuge K., Tanako M., Takeda Y. and Sato M., **J.Phys. Soc. Japan** 57, 1887 (1988).
5. Badalyan A.G., Baranov P.G., Aleksandrov V.I., Borik M.A. and Osiko V.V., **Pis'ma Zh.Eksp.Teor.Fiz.** 49, 606 (1989).
6. Shaltid D., Barnes S.E., Bill H., Francois M., Hagemann H., Jegondaz J., Lovy D., Monod P., Peter M., Revcolevschi A. and Sadowski W, **Physica C** 161, 13 (1989).
7. Pop A.V., Nicula Al., Darabont Al., Giurgiu L.V., **Procc.RAMIS Conference (Poznan),** 264 (1989).
8. Deville A., Gaillard B., Bejjit L., Monnereau O., Noel H. and Potel M., Physica B 165-166, 1319 (1990).
9. Janossy A., Rockenbauer A., Pekker S., **Physica C** 167, 301 (1990).
10. Nicula Al., Pop A.V., Giurgiu L.V., Darabont A. and Cosma I. (Stuttgart), 284(1990).
11. Kanoda K., Takahashi T., Kawagoe T., Mizoguchi T., Kagoshima S., and M.Hasumi, (1987).

STUDIA UNIV. BABEŞ-BOLYAI, PHYSICA, XXXVI, 2, 1991

SPECTROSCOPY OF LASER PRODUCED PLASMA FROM $YBa_2Cu_3O_{7-x}$ CERAMICS

V.A.BUDYANU[1], I.A.DAMASKIN[1], S.A.FEDOSEEV[1], S.L.PYSHKIN[1], Val.P.ZENCHENKO[1], Vit.P.ZENCHENKO[1]

ABSTRACT. In the work the main parameters and characteristics of laser produced plasma from Y-Ba-Cu-O ceramics were systematically investigated. It has been observed that depending on laser irradiation density power for the superconductive ceramics there are three various evaporation regimes. Interdependence between the evaporation regime of a target and composition of the obtained films is discussed.

1. INTRODUCTION. Now laser vacuum deposition (LVD) is widely used for fabrication of HTC-films on various substrates[1-3]. Superconductivity of the named structures depends on the two factors such as substrate material as well as deviation of the film composition from stoichiometry. Optimization of LVD in the case of stoichiometric HTC-film fabrication is rather difficult problem due to complicated chemical composition of HTC-materials as well as large number of the technological parametres guiding the LVD method. Some additional complications are arising due to the poor information on the based parameters of vapor-plasma fluxes produced in laser evaporation of HTC-targets.

The present paper deals with the results on spectroscopy of intrinsec irradiation of laser produced plasma from HTC-ceramics on the base of Y-Ba-Cu-O composition. Analysis of the space and temporally resolved irradiation spectra gives good opportunity to find some important parameters and features of laser produced plasma as well as to use them for the optimization of the LVD method for HTC-film deposition.

---

[1] *Institute of Applied Physics, Moldova Acad.Sci., Chişinău.*

2. EXPERIMENTAL SET-UP. The experimental set-up included vacuum chamber (~10^{-8}Pa), Nd^{3+}-glass laser (pulse duration-30 ns, pulse energy-0.5 J, repetition rate-2+3 Hz) and some system for registration of the laser plasma irradiation. The optical axis of the monochromator (the reciprocal linear dispersion is 1.3 nm/mm) was oriented perpendicular to the movement direction of the plasma flux. An image of the latter with the help of a lense system having a small depth of focus was projected on the input slit of the monochromator. PMT connected with the input of an one-channel boxcar-integrator provided the recovery of a signal in a given time interval. For the control and observation of the signals memory oscilloscopes were used. The scheme of the registration was externally triggered with the help of the Nd-glass laser pulses registered by a fast photodiode. Using such installation one can investigate the laser plasma irradiation in 0.35+1 μm spectral region at the distance from the target from 0.2 to 5 cm (space, time and spectral resolution were 10^{-4} cm^3, 2 ns and 0.1 A respectively).

3. EXPERIMENTAL RESULTS. The laser plasma was produced by laser evaporation of flat targets from HTC-Y-Ba-Cu-O ceramics. The laser power density W on the target was varied within the interval from 30 to 3000 MW/cm^2. The vapour-plasma flux spectrum has lines of neutral atoms as well as singularly charged ions against a background of a continous spectrum. For the investigation of both structure and dynamics of scattering of the

flux we used the following spectral lines: 4653(YI) 4691(BaI), 5218(CuI),3692(OI), 3594(YII), 3891(BaII), 4227(CuII) and 4319(OII) A. The fulfilled investigation showed that there are three various regimes of Y-Ba-Cu-O-ceramics evaporation.

At $W < W_1 = 5*10^7$ W/cm^2 there appears laser plasma of low density. The irradiation both of excited atoms and ions in the plasma decay completely at 0.01÷0.1 cm from the target. There is no possibility to register the characteristic irradiation both of atoms and ions at such distances due to high intensity of continous background. Spectra of masses for this evaporation regime show that in the vacuum chamber there are some quantity of atoms constituted of the ceramics as well as some oxides of those elements.

Within the interval $W_1 < W < W_2 = 2.5*10^8$ W/cm^2 there appears the plasma which is more dense, then in the previous case, that results in arising some effective chanels of additional excitation both of atoms and ions. At the distances 0.2 ÷5 cm from the target, where the irradiation of neutral and ionized atoms was just registered, intensity of background irradiation was only nearly 10% of the intensity of spectral lines. At fixed distances from the targets time dependences of the irradiation intensities both of the atoms and ions have the hump-like shape. A change of the shape during the flight of the plasma flux between the target and the substrate is bound up with broadening of the plasma flux.

As it follows from the Fig.1, the above pointed change is various for heavy (Y,Ba) and light (O,Cu) atoms. Probably, these

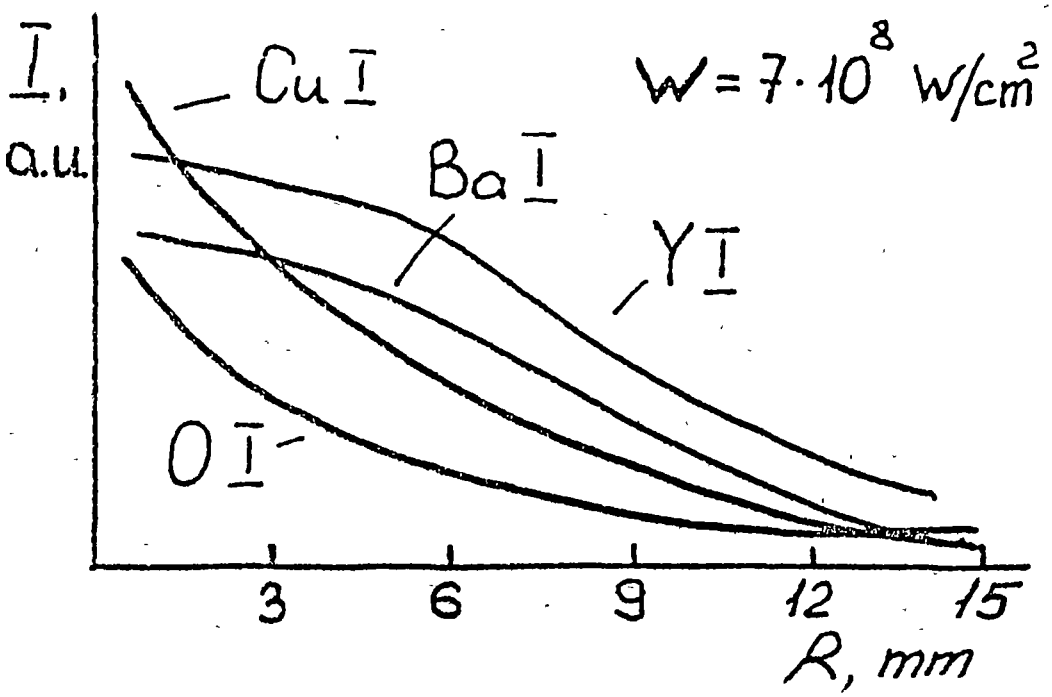

Figure 1. Irradiation intensity of the laser plasma components as a function of the distance from the target.

differences may result from various mechanisms of flux broadening -linear for, Y, Ba atoms and three-dimensional for the light atoms. This conclusion can be confirmed from the analysis of the spectral line shapes. The evaluation shows that at small distances from the target the width of atomic lines is a function of the resonance atomic collisions, but the width of ions lines

depends on the intensity of the Holtz-Markov interaction. In these mechanisms the line width is proportional to the density of particles of given type as well as to ion density respectively. So we can investigate both the structure of the vapour-plasma fluxes as well as their evolution in the flight between the target and the substrate.

From Fig.2 one can see that the dependence of half-width of the spectral lines $\Delta\lambda$ on distance R can be expressed as $\Delta\lambda \sim R^{-n}$, where n=1 for YI and n=2+3 for Cu(II). Thus, the broadening of the flux of YI atoms has one-dimensional character, while the broadening of the cluster of CuII is three-dimensional. Comparing calculated and measured widths of the spectral lines one can conclude, that the density of neutral particles at 0.2+2 cm distance from the barrier (substrate) changes from 10^{19} cm^{-3} till 10^{-3}. The density of ions in the same space interval changes from 10^{18} cm^{-3} till $(1\div10)*10^{16}$ cm^{-3}. The Doppler-type interaction gives the main contribution into the broadening of spectral lines at the distances greater than 2 cm.

The further increase of laser power on the target ($W > W_2$ leads to the changes in the structure of the fluxes as well as in energy distribution of atoms and ions. Fig.3 show the transition from regime $W<W_2$ to $W>W_2$. It is seen from the Fig.3 that at $W>2.5*10^8$ W/cm^2 the second hump appears on the temporal profile of the irradiation intensity. Note, that the energy distribution is essentially non-equilibrium. In the plasma flux we find gast and slow components. We can see that in initial stage of the plasma movement the fast component further

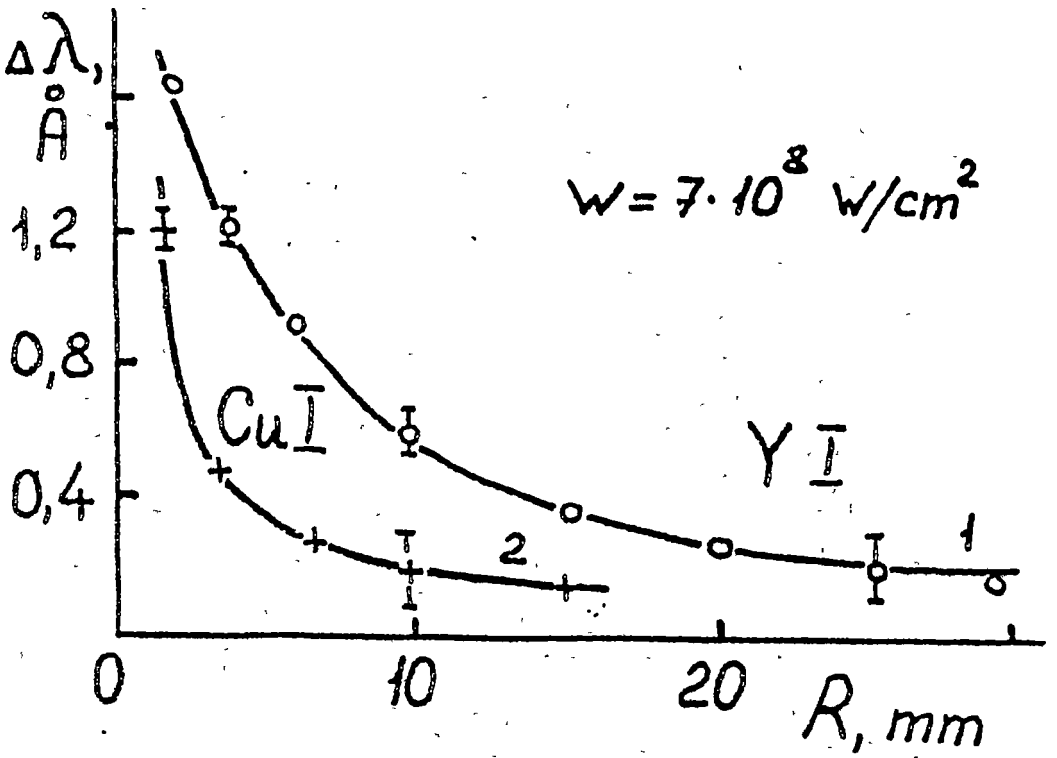

Figure 2. The dependence of the halfwidth of YI(1) and CuI(2) on the distance from the target.

accelerates while the one looses its speed.

For the purpose of the optimization of the technological processes in the vacuum chamber the pressure of oxigen was changed and the dependence of half-width on its pressure has been investigated. Fig.4 shows that at some distance from the target, which changes depending on oxygen pressure, the half-width of the

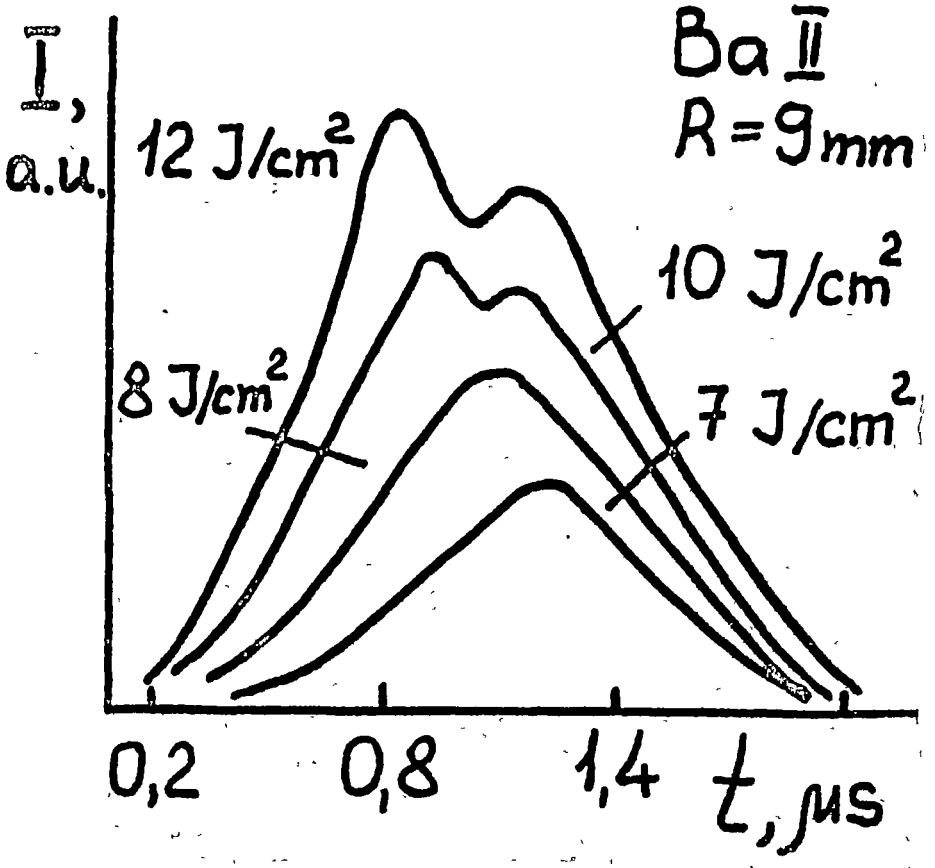

Figure 3. Time dependences of the irradiation intensity for Ba II line at various density of laser power on the target.

line is a function of intensity of collisions between the evaporated target particles and oxigen molecules. In these conditions in discontinuos spectrum of the laser plasma some additional lines appear, which may be associated with the Y,Ba or Cu-oxides. Thus, depending on oxigen pressure in the chamber as well as on the distance from the target one can observe the

transition from the inertial scattering of atomic fluxes to the oxigenization regime.

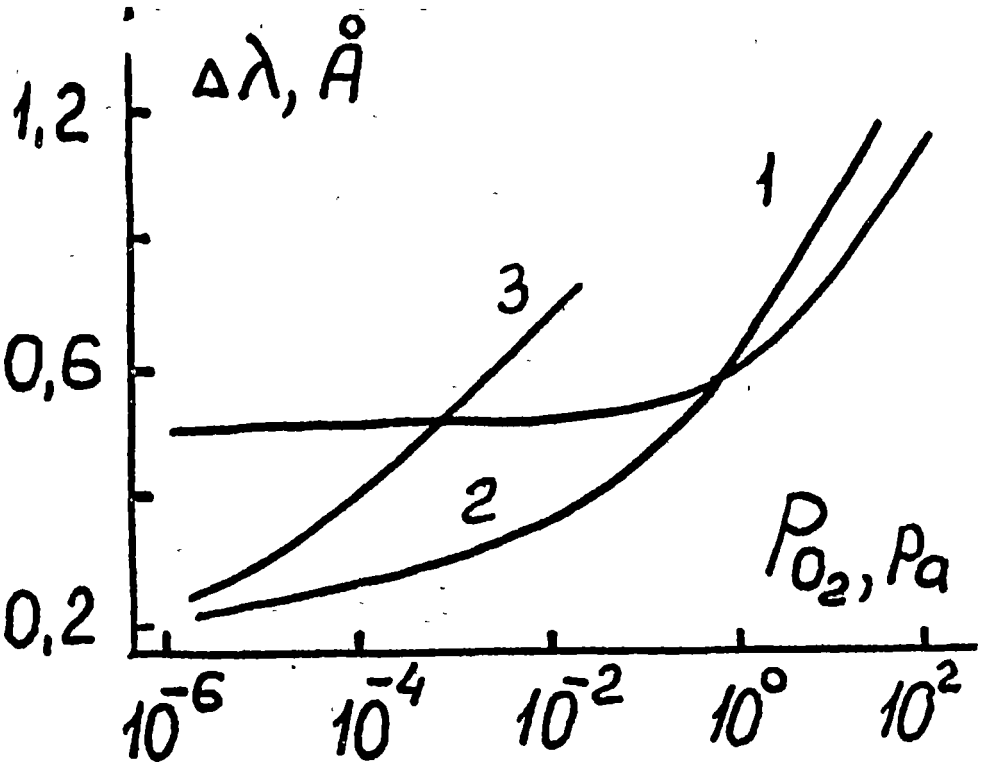

Figure 4. The dependences of half-width of BaI spectral line (λ=4691 A) on residual pressure of oxigen in the chamber at various distances R from the target: 1.R=9 mm; 2.R=20 mm; 3.R=30 mm.

4. CONCLUSION. Thus, three various regimes of laser evaporation of the ceramics have been established. These regimes differ each other in parameters of the plasma fluxes. Respectively there are essential diferences in the film composition. Particularly, the layer by layer Augier-analysis show some considerable deficit of Cu at $W>W_1$, while at $W>W_2$ we also found the deficit of Y. The effect can be connected with the local deviation from the stoichiometry on vapour-plasma fluxes, due to the various character of cluster broadening in the case of light or heady atoms as well as with rather high intensity of ion component at $W>W_1$. Films with the composition close to the 1:2:3 ratio was prepared at $W<W_1$.

REFERENCES

1. Dijkkamp D.,Venkatesan T., Wu X.D. at al. Preparation of Y-Ba-Cu oxide superconductor thin film using pulsed laser evaporation from high T_c bulk material. Appl.Phys.Lett., 51, 619-621 (1987).
2. Wu X.D., Dijkkamp D., Ogale S.B., at al. Epitaxial ordering of oxide superconductor thin films on (100) $SrTiO_3$ prepared by laser evaporation. Appl.Phys.Lett., 51, 861, (1987).
3. Kwok H.S., Mattocks P., Shi L. at al. Laser evaporation deposition of superconducting and dielectric thin films. Appl.Phys.Lett., 52, 1925 (1988).

STUDIA UNIV. BABEŞ-BOLYAI, PHYSICA, XXXVI, 2, 1991

"PEAK-EFFECT" IN HIGH-T_c SUPERCONDUCTING CERAMICS

L. MIU[1]

The transport critical-current density J_c of superconducting oxide bulk sintered samples is rather low and decreases strongly with applied field H/1,2/. The problem especially lies in the granular nature of polycristalline bulk materials, grain anisotropy, a remarkably short coherence length and large grain boundaries resistance, which cause J_c to be a few orders of magnitude less than the critical-current density inside the grains. The $J_c(H)$ dependence at low H was interpreted in terms of the 'weak-link' model /3/, where the decreases of J_c as 1/H observed for some ceramic samples results directly from the well known Fraunhofer-like diffraction pattern of a single Josephson junction

$$J_c(H) = J_c(0)\ \sin(\pi H/H_o)/\pi H/H_o \qquad (1)$$

with the characteristic field H_o given by

$$H_o = \Phi_o[\mu L(2\lambda+t]^{-1} \qquad (2)$$

where Φ_o is the magnetic flux quantum, μ is the permeability, L is the junction length, λ is the London penetration depth, and t is the barrier thickness. An averaging over angle and junction area gives a field dependence slightly faster than 1/H. As was recently shown /4/, the intergrain weak links are better described by an Airy current-field pattern, which leads to $J_c \alpha H^{-3/2}$ upon averaging.

On the other hand, our experimental results concerning the

---

[1] *Institute of Physics and Technology of Materials, P.O.Box MG-7 Măgurele-Bucharest, Romania.*

modifications induced in the temperature variation of J_c by a small field /5,6/ seem to be consistent with the contribution of thermally activated flux-creep at grain boundaries to J_c reduction in ceramics, at least at high temperatures.

In certain cases, a maximum in $J_c(H)$ at relatively low field values was observed /7,8/. It is very difficult to explain this behaviour with the widely accepted weak-link model. The investigation of the nature of such a peculiar effect may give new information about the actual limiting factors of J_c in ceramics.

Transport critical-current measurements $I_c(H,T)$ and magnetization studies performed by us on Bi-based ceramics and 123 bulk sintered materials revealed the following aspects:

a) At low H, $I_c(H)$ has the form

$$I_c(H) \alpha H^n \qquad (3)$$

where the exponent n depends on the path in the (h,T) diagram /9/. In zero-field-cooling (zfc) conditions and increasing field n=-1, whereas, in field-cooling (fc) conditions, n=-0.8 ÷ - 0.5.

b) The temperature dependence of H_o near T_c for Bi-based 2223 samples was found to be much slower that in Eq. (2) /5/.

c) The peak-effect mainly appears in zfc conditions and increasing field /8/.

d) With decreasing temperature, the I_c minimum becomes more pronunced and shifts its position to higher H values.

e) The peak-field H_p increases at low temperatures.

f) The field H_v corresponding to I_c minimum and the field H_m at which the absolute value of the shielding magnetic moment of

the sample is maximum are connected. H_v is always slightly higher than H_m.

The experimental facts a), c),d) and f) suggest the role of demagnetization effects, at least at low H. For $H \sim H_m$, in the conditions of imperfect grain diamagnetism, but far enough from complete critical-state penetration, a simple analysis of the effective field $H^{eff}(H)$ experienced by the contact between two grains gives (in the case of our low mass-density samples)

$$H^{eff}(H) = H + 4\pi(\rho_t/\rho_s)|M(H)| \quad (1+D_g)/(1-D_g), \qquad (4)$$

where ρ_s is the sample mass-density (=3.9 g/cm^3), ρ_t-the X-ray mass-density, M(H) -the sample magnetization, and D_g is the grain demagnetizing factor. Due to the low J_c values at fields of the integrain currents to the diamagnetic signal of the sample was neglected. SEM studies revealed in the case of Bi-based flat crystallites which can be approximated as thin disk of mean diameter Φ=4 μm and heigth h~0.5 μm, implying a value $D_g=1-(\pi/2)(h/\Phi)=0.8$ in perpendicular field. The degree of preferential crystallite orientation is not very important here, the irreversible magnetization having a large component parallel to the c direction whatever the field orientation, except for angles very close to the (a,b) plane /10/. A grain demagnetizing factor close to unity associated with effective pinning barriers to flux entry may le\ad to H^{eff} values appreciably higher than H and, consequently, an important supplementary factor for the $I_c(H)$ decreases in the low applied field range appears.

Assuming now that the transport critical-currewnt is a decreasing function of the effective field at the intergrain

contacts, it is clear that the demagnetization effects should lead at most to a plateau in the $I_c(H)$ dependence, starting at an applied field value slightly higher than H_m (see Eq.(4)). This is in agreement with f). However, in the conditions of continuous flux penetration inside the grains, for 'usual' pinning barriers, H^{eff} always increases with H and; in order to explain the I_c increase at $H>H_v$, we must reconsider the problem of J_c limitation in ceramics.

Besides weak links quenching, the temperature dependence of the transport critical-current density in low magnetic field /6/ indicated the weak intergranular pinning as one of the limiting factor for J_c in ceramics. In this situation, the I_c increase at $H>H_v$ may occur from an enhancement of the intergranular pinning in the field domain where the intragranular pinning force increases, through vortex-vortex interaction. I_c starts to increase in the field range where there is a huge flux penetration inside the grains /8/.

All the features of this new type of peak-effect corroborate with the above considerations. The decrease of the valley field at high temperatures is caused by the reduction of the absolute value of the grain magnetization at H_m, which appears due to integrain pinning weakening and to the decreases of the lower critical field of the grains. Also, the significant changes in the M(H) dependence observed in fc conditions or in decreasing field lead to the diminutions of the effect. The increase of H_p at low temperatures appears naturally since both the Josephson upper critical field and the intragranular 'irreversibility-

field' increase.

Finally, it is worth noting that the low voltage level I-V characteristics of our samples can also be described in terms of thermally activated flux-creep at grain boundaries, following /11/, but with a transport-current density dependent pinning energy barrier /12/.

In conclusion, in our opinion, there is a supplemental limiting factor for J_c in ceramics: the existence of weak intergranular pinning regions in the bulk sintered materials.

REFERENCES

1. Kwak J.F. et al., **Phys. Rev. B 37**, 9749 (1988).
2. Hampshire D.P. et al., **Supercond. Sci. Technol. 1**, 12 (1988).
3. Peterson R.L.and Ekin J.W., **Phys. Rev. B 37**, 9848 (1988).
4. Peterson R.L. and Ekin J.W., **Physica C 157**, 325 (1989).
5. Miu L. et al., **J.Mat. Sci. Lett. 9**, 532 (1990).
6. Miu L. et al., **J. of Superconductivity 3**, (4), 391 (1990).
7. Thompson J.R. et al., **Phys. Rev. B 39**, 6652 (1989).
8. Miu L. et al., (submitted).
9. Miu L., **World Sci. 21**, 586 (1990).
10. Fruchter L. et al., **Physica C 160**, 185 (1990).
11. Miu L. and Popa S., **J. Low Temp. Phys. 42**, 203 (1981).
12. Miu L. and Crisan A.,(to be published).

STUDIA UNIV. BABEŞ-BOLYAI, PHYSICA, XXXVI, 2, 1991

ON THE SUPERCONDUCTING CRITICAL TEMPERATURE OF $La_{2-x}Ba_xCuO_4$

Liliana MACARIE[1], Lida VASILIU-DOLOC[1], F. BUZATU[1] and M. APOSTOL[1]

ABSTRACT. The supercondcuting critical temperature o $La_{2-x}Ba_xCuO_4$ is analyzed by making use of the interaction between the charge carriers and the oxygen-displaciv mode of the lattice. The possible change in the electronic structure is investigated as arising from the structural model is proposed which may explain the dependence of the critical.

1. INTRODUCTION. The high-temperature superconductivity with the onest critical temperature near 30 K has been discovered[1] in the La-Ba-Cu-O system. The superconducting phase $La_{2-x}Ba_xCuO_4$[2] belongs to the La-based class of superconductors with the general chemical formula $La_{2-x}M_xCuO_4$, $0<x<0.3$ and slight oxygen deficiency, where M=Sr[3,4] (highest critical temperature in the class, near 37 K), M=Ca[5] and M=Na[6]. The semiconducting parent compound La_2CuO_4 has an orthorhombic (distorted) crystalline structure of the K_2NiF_4-type over all the available temperature range[7-9] while the M doping has the effect of stabilizing the tetragonal phase towards higher temperatures[10]. The most studied member of the class is the M=Sr compound which possesses an orthorhombic crystalline structure at low temperatures for $x\leq 0.2$ and exhibits no direct correlation between the tetragonal-orthorhombic transition and the superconducting properties. The critical temperature has been shown to depend essentially on the Sr content x as well as the oxygen deficiency, both parameters contributing to the concentration of the charge carriers. A maximum critical temperature ~37 K is reached for an optimum Sr content $x_o \approx 0.15-0.2$.

---

[1] *Institute of Physics, Măgurele-Bucharest, P.O.Box MG 6, Romania.*

It has been put forward[11,12] that the superconductivity in the high-temperature superconductors would originate in the interaction of the charge carriers with the oxygen-displacive modes of the lattice. This theory may account for the high values of the critical temperature of Y-based superconductors (123 class)[13], Bi(Tl)-based superconductors[14] and 124 class of superconductors[15] as well as for the isotope shift and the superconducting gap[16]. In particular the x dependence of the critical temperature is obtained in fair agreement with the experimental data for $La_{2-x}Sr_xCuO_4$[16,17].

The superconductor $La_{2-x}Ba_xCuO_4$ exhibits some particularities in comparison with $La_{2-x}Sr_xCuO_4$, among which a two-maxima x-dependence of the critical temperature[18] and an additional orthorhombic-tetragonal transtition towards lower temperatures[19]. These two questions are addresed in the present paper within the frame of the superconductivity mechanism based on the interaction between the charge carriers and the oxygen-displacive modes of the lattice. It is shown that the aforementioned orthorhombic-tetragonal transition may change the Brillouin zone of the compound in such a way as to strongly depress the critical temperature at x=0.125, exactly as observed experimentally. The critical temperature obtained by using this electronic structure model exhibits two maxima located near x=0.1 and x=0.15, in agreement with the experimental data.

General structural and superconducting properties of $La_{2-x}Ba_xCuO_4$ are given in section 2, the critical temperature is analyzed in section 3 and the results and discussion are given

in the last section of the paper.

2. STRUCTURAL AND SUPERCONDUCTING PROPERTIES OF $La_{2-x}Ba_xCuO_4$.

The tetragonal crystalline structure of $La_{1.8}Ba_{0.2}CuO_4$ has been studied by X-ray diffraction[20] and a soft-mode lattice instability has been pointed out for $La_{1.85}Ba_{0.15}CuO_4$ by neutron scattering experiments[21]. Neutron scattering studies of $La_{1.85}Ba_{0.15}CuO_4$ have also revealed a tetragonal-orthorhombic transition below 180 K and a subtle strucutral anomaly: unlike the M=Sr compound[23] the orthorhombic splitting has a marked decrease below 75 K which saturates around the onset superconducting temperature 35 K and is accompanied by a plateau or gentle rise in the resistivity-versus-temperature curve just above this onset superconducting temperature. Some other anomalies have been reported in the thermal[24], elastic[25,26], optical[27] and transport[18,28] properties of $La_{2-x}Ba_xCuO_4$ which, in contrast with the M=Sr compound[23], seem to indicate a direct correlation between the structural changes undergone by this compound and its superconductivity properties.

Unlike the M=Sr superconductor[16,17] the critical temperature T_c versus Ba concentration x has two maxima $T_c^{max}\simeq 26$ K (magnetic measurements) located near $x\simeq 0.1$ and $x\simeq 0.15$ with an in-between minimum of, probably, vanishing T_c at $x\simeq 0.125$[18]. Samples with $x=0.12$ and $x=0.2$, having a low bulk transition T_c, exhibit an additional incipient transition with an onset near 30 K (resistance measurements)[18], which seems to indicate the presence of two superconducting phases; and samples with $0.1<x<0.15$

exhibiting strongly depressed critical temperatures show a plateau or gentle rise in the resistivity-versus-temperature curve just above the onset superconducting temperature[18], which suggests an enhanced localization of the change carriers.

A tetragonal-orthorhombic transition has been reported for $La_{2-x}Ba_xCuO_4$ over all the available x range below temperatures decreasing from 400 K for x≈0.05 to~70 K for x≈0.18[19]; in addition, low-temperature tetragonal phase of a particular symmetry has been pointed out[19] for 0.05<x<0.15 below temperatures which increase up to~80 K and then slightly decrease with increasing x. The phase diagram of these various structural phases[19] shows that the superconductivity of $La_{2-x}Ba_xCuO_4$ occurs in the orthorhombic phase for 0<x<0.05 and in the low-temperature tetragonal phase for 0.05<x<0.15. The low-temperature tetragonal phase may induce such changes in the electronic structure as to affect drastically the superconducting critical temperature, at least for some values of the parameter x.

3.SUPERCONDUCTING CRITICAL TEMPERATURE. The theory of the interaction between the charge carriers and the oxygen-displacive modes of the lattice[11,12,16] derives the high-temperatuire mechanism of superconductivity from the coupling of the Cu-3d-O-2p strongly hybridized electronic orbitals with the oxygen-displacive modes of the layers of Cu-oxygen aggregates (octahedra, pyramids, rhombohedra). Both an on-site and inter-site Jahn-Teller-type of coupling leads to an extended model of molecular solid, with the in-layer electronic motion governed by

a two-dimensional Hubbard hamiltonian, which, under certain circumstances, may exhibit an effective attraction between the charge carriers strongly distorting their lattice environment (small polarons). A Cooper-type pairing hamiltonian may then be exctracted which leads to a critical temperature (gap) equation of the classical BCS-type.

$$\Delta_k=\sum_{\sigma k'} V_{kk'}(\Delta_{k'}/2\varepsilon_{k'})\tanh(\beta_c\varepsilon_{k'}/2) \qquad (1)$$

In equation (1) Δ_k is the gap param,eter of in-plane wavevector k and β_c is the reciprocal critical temperature; $V_{kk'} = (2J^*/N)v(k-k')$ is the pairing potential, where J' is the effective strength (Coulomb repulsion including) of the attractive interaction and N is the number of Cu sites in the Cu-oxygen layer; one-particle (spin σ) energy levels are given by $\varepsilon_k = tv(k)$, where t is the renormalized (polaronic) bandwidth parameter; and $v(k) = 4\cos(ak_x/2)\cos(ak_y/2)$ corresponds to a square lattice of constant a with two inequivalent Cu sites per unit cell as in the case of an orthorhombic structure or an antiferromagnetic ordering (orthorhombic splitting neglected).

The main difference as compared with the standard BCS theory is the extention of the summation in (1) over all the available electronic states. The parameter of relevance in this context is the area S of the Fermi sea related to the filling factor of the Brillouin zone. Assuming a model disc-like Fermi sea of charge carriers (probably holes) states, $x = Cu^{3+}/Cu$ holes per Cu cation (oxygen deficiency neglected) and a gap at the half-filling(x=0) of the band, in accordance with the general data for the high-

temperature superconductors, one obtains $S = (2\pi/a)^2 x$. Averaging the pair potential for the singlet superconductivity over the Fermi sea, $V_{kk'} = (8J^*/N)(1 - \pi x/2)$, (1) reads.

$$1=[(2/\pi-x/\alpha]\ln(2.28\sqrt{3\pi}tx\beta_c),\alpha=t/2J^* \qquad (2)$$

for low values of x (x<0.3) and in the weak-coupling limit (α < 0.506), whence the critical temperature

$$T_c=2.28\sqrt{3\pi}tx\exp(-\alpha/(2/\pi-x)) \qquad (3)$$

is obtained. With the whole caution required by the simplifying approximations made in deriving it equation (3) has been employed in analyzing the dependence of the critical temperature on the hole concentration (x variable in (3)) for $La_{2-x}Sr_xCuO_4$[16,17], Y-based superconductors (123 class)[13], 124 class of superconductors[15] and Bi(Tl) -based superconductors[14]. The main feature of (3) is the prediction of a maximum critical temperature T_c^{max} reached for an optimum hole concentration x_o given by

$$\alpha=(2/\pi-x_o)^2/x_o \qquad (4)$$

The theory of the oxygen-displacive modes has also been developed[14] to speculate on a maximum attainable critical temperature in the whole family of high-temperature superconductors based on layered cuprate oxydes as well as to estimate the presumable effect of the changes in the crystalline structure on the superconducting critical temperature, as in the case of latticial modulations.

The concern here is that of investigating the changes

brought about in the electronic structure of $La_{2-x}Ba_xCuO_4$ by the low-temperature tetragonal phase and their possible effect on the superconducting critical temperature of this compound. The low-temperature tetragonal phase is assumed[19] to consist of a coherent superposition of two types of orthorhombic twins with complementary distortions. One of such distorted orthorhombic block is represented by the dashed area in figure 1, where the smallest-size square is the unit cell of the high-temperature tetragonal phase and the solid circles represent the positions of the Cu-oxygen aggregates. The two types of distortions symbolized by arrows can only be matched into a repeating block by constructing an enlarged and rotated unit cell with respect to the original unit cell of orthorhombic symmetry, as shown in figure 1. This unit cell has an underlying tetragonal symmetry, is 8 times larger than the unit cell of the orthorhombic phase and is $\pi/4$ rotated against the latter. One may tentatively adopt this construction as the unit cell of the low-temperature tetragonal phase. It is now easy to see what is the effect of this new symmetry on the $2\pi/a \times 2\pi/a$ Brillouin zone of the orthorhombic phase, a quarter of which is schematically represented in figure 2 (orthorhombic splitting neglected). The new enlarged and rotated unit cell of the low-temperature tetragonal phase acts as if a lattice modulation of four-fold periodicity sets up along the diagonal axes of the Brillouin zone; consequently new energy gaps open up along directions parallel to these axes which turn out to be zone edges of newly-created Brillouin zones, as shown in figure 2, where the first

quarter Brillouin zone of the new tetragonal structure is represented by the $0\pi/2a\pi/2a$ dashed triangle. One can see from figure 2 that the area of the newly-created Brillouin zone is 1/8 the area of the original Brillouin zone of the orthorhombic phase; it follows that for the filling factor x=1/8 the Brillouin zone of the low-temperature tetragonal phase is completely filled (one recalls that a half-filling gap has been assumed), there being no available states for superconductivity any longer. According to (1) the critical temperature vanishes in this case, in agreement with the local minimum of, probably, zero critical temperature located at x=0.125 as reported experimentally[18]. Making use of this model of electronic structure of the low-temperature tetragonal phase one can attempt to estimate the superconducting critical temperature for values of the filling factor x slightly departing from 1/8. This will be done in the first approximation by assuming that the newly-created energy gaps are not so large as to affect drastically the pairing potential and the one-particle energy levels.

For low values of the filling factor x the pairing excitation processes are not affected by the newly-created zone edges; consequently, for x below a certain value x_1 to be determined later the critical temperature in the new tetragonal phase T_c will have the same expression as that given by (3) for the orthorhombic phase. For $x_1<x<1/8$ the edges of the newly-created Brillouin zone begin to be felt by the pairing excitation processes whose range diminishes gradually as the Fermi surface approaches the Brillouin zone edges. The effective area S left

available for these processes is the difference between the Brillouin zone are $(\pi/\sqrt{2}a)^2$ and the Fermi sea are $S=(2\pi/a)^2-S$, which corresponds to an effective filling factor $x^*=1/8-x$ in a disc-like Fermi sea approximation. Replacing x in (2) by x^* one obtains

$$Tc=2.28\sqrt{3\pi}tx^*\exp(-\alpha/(2/\pi-x^*)),x^*=1/8-x,x_1<x<1/8 \qquad (5)$$

and the continiuty condition between (3) and (5) yields $x_1=1/8-x_1$,

whence $x_1=1/16$. One should remark upon the closeness of this $x_1=1/16\approx0.06$ value, where the low-temperature tertagonal phase may be seen from in the superconducting critical temperature, and the x=0.05 value, where the orthorhombic-low-temperature tetragonal transition begins to be seen experimentally[19]. For the fermi sea transceding the first Brillouin zone only the excess area with respect to this Brillouin zone will be active in the pairing excitation processes (second zone contribution); this excess area S is obtained by subtracting the Brillouin zone area $(\pi/\sqrt{2}a)^2$ from the Fermi sea area $S = (2\pi/a)^2x$, $S = s - (\pi/\sqrt{2}a)^2$, which corresponds to an effective filling factor $x^*=x-1/8$. The active part of the Fermi sea placed now in the second zone can be approximated by two $x^*/2$; this new filling factor should now replace x in (2) where, in addition, a factor 2 occurs in the r.h.s. of (2) as due to the controbution of the two Fermi seas. Therefore, uder these approximations one obtains

$$T_c=2.28\sqrt{3\pi}t(x^*/2)\exp(-(\alpha/2)/(2/\pi-x^*/2)),x^*=x-1/8,1/8<x, \qquad (6)$$

for the critical temperature in this range of x. One should

mention that all the approximations made in deriving both (5) and (6) are valid strictly for x very slightly departing from 1/8; therefore (6) cannot be used for x too far away from 1/8 and (5) may not be valid for x too close to x_1=1/16. The critical temperature given by (3), (5) and (6) is compared with the experimental x-dependence of the critical temperature of $La_{2-x}Ba_xCuO_4$[18] in the next section.

4. **RESULTS AND DISCUSSION**. According to the experimental evidence[18] samples of $La_{2-x}Ba_xCuO_4$ (oxygen deficiency neglected) with low critical temperatures of bulk transition, i.e. with x around 1/8, exhibit systematically an additional incipient transition at a higher onset temperature. We assing this transition to the orthorhombic phase which seems to be of rather little effectiveness in this range of x. According to the magnetic measurement results[18] reproduced in figure 3 (solid circles; triangles correspond to samples whose T_c is not above 4.2 K) the maximum critical temperature does not seem to exceed T_c^{max}=26 k and the incipient transition is located somewhere around 1/8. Indeed, it has clearly been observed[18] a maximum critical temperature 30 K at x=0.12, from electrical resistance measurements. Therefore we shall adopt for the orthorhombic phase T_c^{max}=26 K (in accordance with the magnetic measurement data) located at the optimum Ba concentration x_o=0.12. Under this assumption one obtains the parameters α=2.224 and t=1296 K from (3) and (4) and, using (3), one can draw the $T_c(x)$ curve Oabcd in figure 3, which corresponds to the critical temperature in the

orthorombic phase.

In order to ensure the consistency with the assumptions made in the present theoretical analysis one has to admit the same values of the parameters α and t for the low-temperature tetragonal phase as well, which sounds resonably from a physical viewpoint. By making use, therefore, of α and t fixed above one can plot T_c versus x as given by (5) and (6) and obtain the critical temperature in the low-temperature tetragonal phase as follows:Oa branch for $0<x<1/16$, ae1/8 branch for $1/16<x<1/8$ and 1/8c branch for x slightly beyond 1/8, according to the results of the previous section.

Some comments are in order here. First of all one can see that the two ~26 K maxima observed experimentally[18] near $\simeq 0.1$ and $x \simeq 0.15$ are satisfactorily reproduced by our fit (b and c point in figure 3) as well as the strongly depressed critical temperature at $x=0.125$, which follows as a consequence from the proposed model of electronic structure (the vertical line at $x=1/8$ in figure 3 represents the fully occupied Brillouin zone of the low-temperature tetragonalphase). In addition the narrow range of x around 0.125 where the critical temperature is strongly depressed is consistent with the validity conditions of the theoretical estimations given by (5) and (6) which makes the present analysis to be appropriate.

The two structural phases are not active in the superconducting bulk transitions over the same range of the Ba concentration x. For example, the orthorhombic phase certainly does not contribute for x within a narrow range around 0.125 (bc

dashed piece in figure 3) where the low-temperature tertagonal phase is active. Indeed, plateaux or gentle rises have been reported[18] in the resistivity-versus-temperature curve just above onset critical temperature for $0.1<x<0.15$, pointing toward an anomalous electronic structure; it is noteworthy that exactly in this range the low-temperature tertagonal phase is active in superconductivity (e1/8c solid line in figure 3), the newly-created energy gap being gradually effective in reducing the charge carrier mobility as x is approaching 1/8. The dashed ae line in figure 3 indicates that the low-temperature tetragonal phase gradually loses in effectiveness as x approaches 1/16 from above: for x near 1/16 (the point a in figure 3) either the low-temperature tetragonal phase does not set up yet (according to the structural phase diagram[19] it begins around $x\approx0.05$) or the difference between the two structural phases is not felt by the critical temperature, according to the present theoretical analysis.

For x greater than 0.15 the anomalies in the resistivity-versus-temperature curve disappear[18] which may suggest that the low-temperature tetragonal phase is not longer active in this range. This is consistent with the results shown in figure 3 where one can see that the critical temperature corresponds to the orthorhombic phase for x greater than 0.15. The gradual ineffectiveness of the low-temperature tetragonal phase towards the a and c ends of the x range centered around 1/8 may also suggest that the gap opened by this phase in the electronic structure depends on x and gradually vanishes near $x\approx1/16$ (or

$x \approx 0.05$) and $x \approx 0.15$, again in agreement with the structural phase diagram of the compound.

There are sensible discrepancies in figure 3 between the experimental data and the theoretical critical temperatures for low (<0.05) and high (<0.2) values of x. This commonly occurs for almost all the high-temperature superconductors[13-17]. For low values of charge carrier concentration a higher localization is expected as arising from disorder effects, magnetic correlation, etc. For large values of charge carrier concentration the sample quality deteriorates as crystal defects and other imperfections occur or the solubility limit of dopants is reached. A more refined analysis is needed in these regions in order to account for these phenomena. In addition, the effect of the oxygen deficiency should be included in the theoretical treatment.

REFERENCES

1. Bednorz J.G. and Muller K.A., Z.Phys. B64, 189 (1986).
2. Takagi J., Uchida S., Kitazawa K. and Tanaka S., Jpn. J.Appl.Phys.Lett. 26, L123, (1987).
3. Cava R.J., VanDover R.B., Batlogg B. and Rietman E.A., Phys.Rev.Lett. 58, 408, (1987).
4. vanDover R.B., Cava R.J., Batlogg B. and Rietman E.A., Phys.Rev.B35, 5337, (1987).
5. Bednorz J.G., Muller K.A. and Takashige M., Science 236, 73, (1987).
6. Markert J.T., Seaman C.L., Zhou H. and Maple M.B., Solid St.Commun.66, 387 (1988).
7. Longo J.M. and Raccah P.M., J.Solid St.Chem. 6, 526 (1973).
8. Grande V.B., Hk.Muller-Buschbaum and Schweizer, Z.Anorg.Allg.Chem. 428, 120 (1977).
9. Singh K.K., Ganguly P.and Goodenough J.B., J.Solid St.Chem. 52, 254 (1984).
10. Michel C. and Raveau B., Rev.Chim.Min. 21, 407 (1984).
11. Apostol M., in Proc.Adriatico Res.Conf. on High-Temp.Supercond.,eds. S.Lundquist et al (World Sci., Singapore, (1987) p.309. [Int.J.Mod.Phys. B1, 957 (1987)].

STUDIA UNIV. BABEŞ-BOLYAI, PHYSICA, XXXVI, 2, 1991

DC-MAGNETRON SPUTTERING GUN FOR HTcS THIN FILMS DEPOSITION

T. PETRIŞOR[1], L. CIONTEA[2] and A. GIURGIU[1]

ABSTRACT. An off-axis dc magnetron sputter system operating under high gas pressure conditions has been developed for the in-situ fabrication of high Tc YBCO thin films. The described apparatus enables a stoichiometric deposition at a rate of aproximatively 0.1 nm/s resulting a uniform, smooth and shiny film over a 2.5 cm^2 area. Revelance to practical application is briefly discussed.

1. INTRODUCTION. Deposition of high temperature superconducting thin films presents a great importance for fundamnetal atudies as well as for their potential applications in microelectronics and computers, sensors, energy storage, etc. Various deposition techniques have been used for this purpose including multi-sources ion beam deposition (1, 2), pulsed laser evaporation (3, 4, 5), rf and dc sputtering (6, 7, 8, 9) metal-organic deposition (10, 11) chemical vapor deposition (12, 13) and the screen printing method (14, 15). Most of the thin films obtained by these methods exhibit higher critical currents than the bulk material and comparative critical temperatures (the critical temperature is strongly affected by the nature of the substrate material).

The development of thin films for superconductive applications places specific requirements upon the films. Among these are: reproducible deposition procedures, smooth and uniform film surfaces, superconductivity at the thin film surface and homogeneous deposition on sufficiently large surfaces to allow

[1] Polytechnic University, Physics Department, Str. C.Daicoviciu nr.15, 3400 Cluj-Napoca, Romania.

[2] Polytechnic University, Chemistry Department, Bd-ul Muncii nr.105, 3400 Cluj-Napoca, Romania.

fabrication of complex electronic circuits.

Sputtering meets the above mentioned requirements. In addition, because of the higher kinetic energy of the sputtered flux, sputter-deposited adatoms have higher mobilities than do evaporated atoms. As a result it should be possible to obtain epitaxial films at much lower substrate temperatures than those obtained by other methods.

Among the different sputtering techniques, dc-magnetron sputtering offers additional advantages as preserving the target stoichiometry on the deposited film, small dimensions of the target, low target power density and in-situ film preparation. Under ion bombardment both yttrium and barium are intense secondary electron emitters, which makes the magnetron sputtering technique adequate for high deposition yields. The main disadvantage of this method is caused by the negative ion effect determining significant resputtering from the substrate and hence a low deposition rate (16). In order to eliminate this effect, an off-axis arrangement is generally used.

We report an off-axis dc-magnetron sputtering apparatus for in-situ HTcS thin films deposition, operating under high gas pressure conditions (O_2+Ar between $3\text{-}6*10^{-1}$mbar).

2. EQUIPMENT DESCRIPTION. Atoms are ejected from the surface of any material bombarded by ions or atoms of sufficient energy - this phenomenon is called sputtering and it offers the basis for all the sputtering equipments e.g. rf and dc sputtering, ion beam sputtering, etc. As suggested by Stark (17), sputtering can be

described in the lmits of momentum transfer from bombarding ion to atoms in the target.

The designed equipment is based on a cathodic sputtering and uses a planar cathode magnetron (the cathodic sputtering consists in the ejection of the atoms from the cathode as a result of its striking by the positive ions generated in a low pressure glow discharge).

The cross-section of the cathode magnetron gun is presented in figure 1. Our basic unit is a planar dc magnetron with 15 mm in diameter. This magnetron was built for small diameter targets. The magnet is incorporated behind the target to concentrate the plasma in a region close to it. In the present design the discharge plasma ring diameter is about 20 mm.

A part of the energy is transformed into heat at the impact of the incident ions with the cathode, causing the excesive heating of the target. This fact damages the target and decreases the sputtering yield. For these reasons the target cooling is required. The magnetron gun is equipped with a water cooling is system. For a good heat transfer between the target and the cooling system, the target is glued to the cathode with silver conductive adhesive (ICHIM-Cluj). Argon is injected in the discharge region through the space between the cathode and the magnet, so that the discharge takes place mainly in argon atmosphere.

The anode is a planar copper disk of 30 mm diameter facing the cathode (on-axis). The distance between the cathode and the anode can be adjusted to concentrate the plasma and to optimize

the sputtering yield.

In order to obtain in-situ superconducting thin films, the substrate must be heated during deposition. The heating-holding system is presented in figure 2. The substrate is resistance heated by means of kanthal wire inside the ceramic substrate holder. A Pt-PtRh 18 ther-mocouple, directly attached to the substrate, is used for temperature measurement. The temperature is controlled with a self-made bipositional electronic regulator using the same thermocouple.

Traditionally, the substrate is facing the target (on-axis) since this would result in the fastest film growth rate. However, initial attempts using this orientation and low pressure produce poor quality produce stoichiometric proved to be a tedious process.

A method for correcting the film stoichiometry is to increase the background pressure during the deposition. For YBCO system the simple increase of the background pressure is not enough for successfully producing stoichiometric films. In the case of YBCO negative oxygen ions are formed. These ions are accelerated at full cathode potential toward the substrate which is facing the target in the on-axix arrangement bombarding the growing films. The bombardment of these energetic negative ions produce a selective resputtering of the deposited film with consequences on its stoichiometry.

A solution to these problems has been proved to be the high pressure in-situ off-axis deposition. In off-axis geometry (figure 3) the heater-holder is placed outside the region of

direct on-axis negative ions flux, but within the edges of the plasma region. As a result of this off-axis geometry the atoms that impinge on the substrate are exclusively low energy sputtered neutral atoms that have reached the substrate by diffusion. In this case the film stoichiometry matches the target.

During the deposition oxgygen is sprayed directly on the film to induce a reactive deposition.

The whole above described assembley is placed inside a conventional vacuum system.

3. OPERATING CONDITIONS AND RESULTS. In our sputtering experiments we have used a YBCO target disk of 30 mm in diameter and 2 mm thickness of 1:2:3 stoichiometry. The distance betwen the anode and the cathode is about 40 mm. The gun was operated in the dc mode with a current of 100 mA and a voltage of 400 V in an Ar/O_2 mixture with the partial pressure of $3*10^{-1}$ mbar and $2*10^{-1}$ mbar respectively. In these discharge conditions the plasma ring has a diameter of 20 mm.

The holder-heater was located in an off-axis arrangement, at a distance of 20 mm with respect to the system axis. The substrate was heated up to 700°C (±10°C). The deposition rate is about 0.1 nm/s, resulting a uniform, smooth and shiny film over a 2.5 cm^2 area. The maximum thickness variation of the film was estimated at 15% using optical interference methods.

The superconducting properties of the as deposited thin films will be published elsewhere.

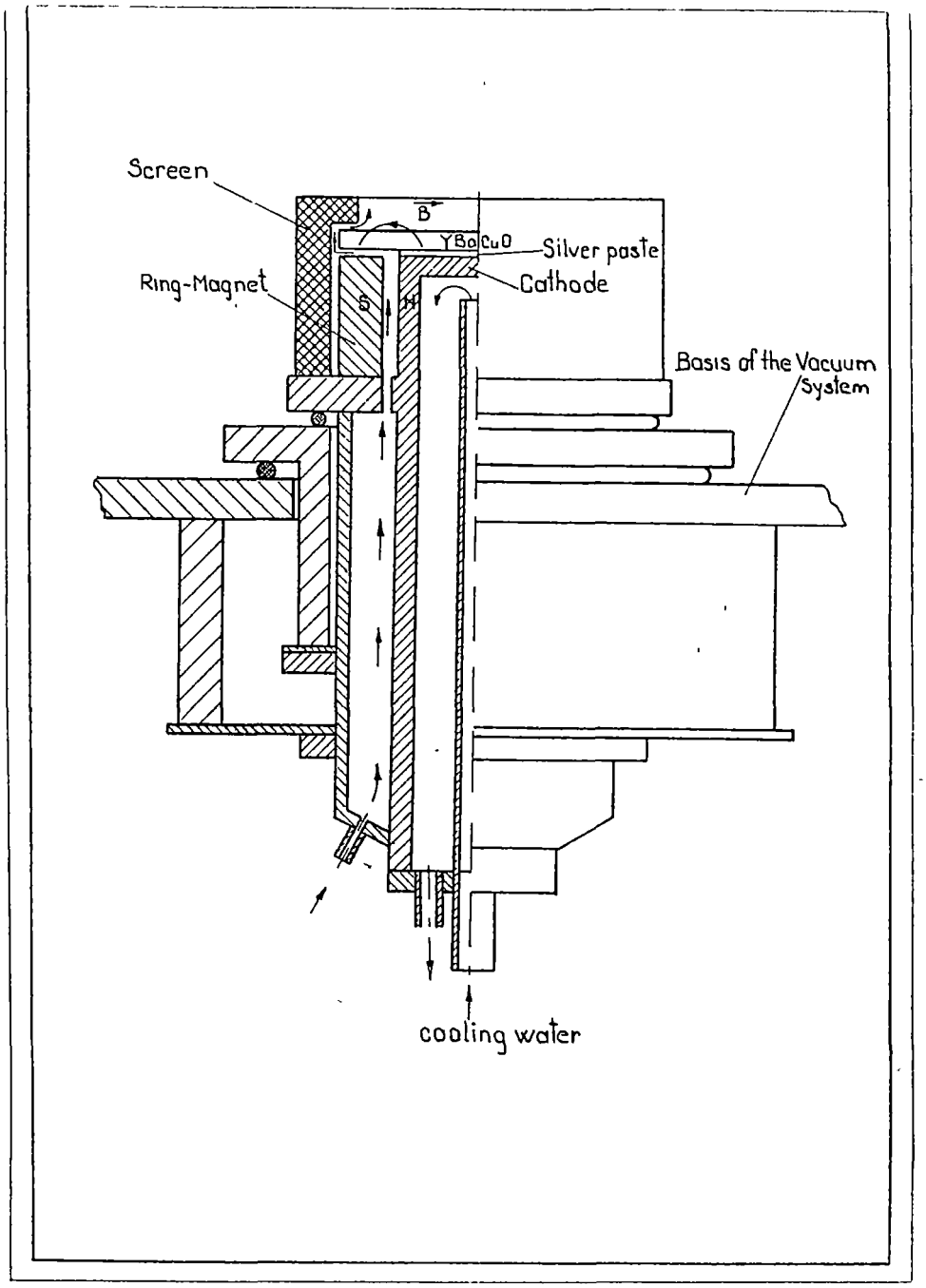

Fig 1. THE EROSS-SECTION OF THE CATHODE MAGNETRON GUN

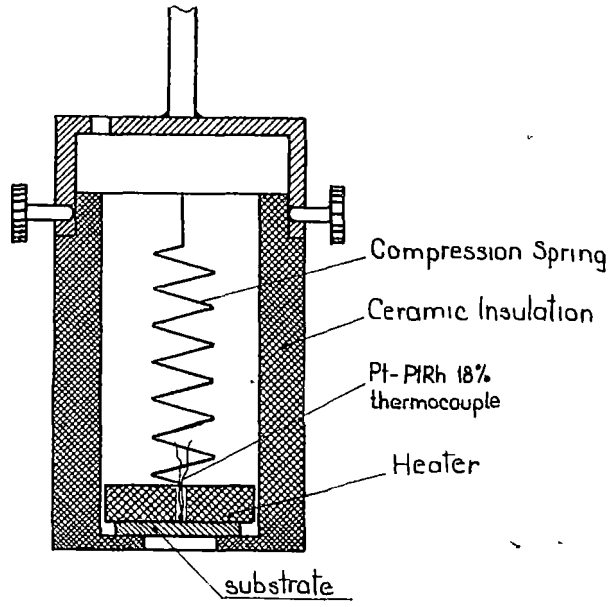

Fig. 2. THE HEATING - HOLDING SYSTEM.

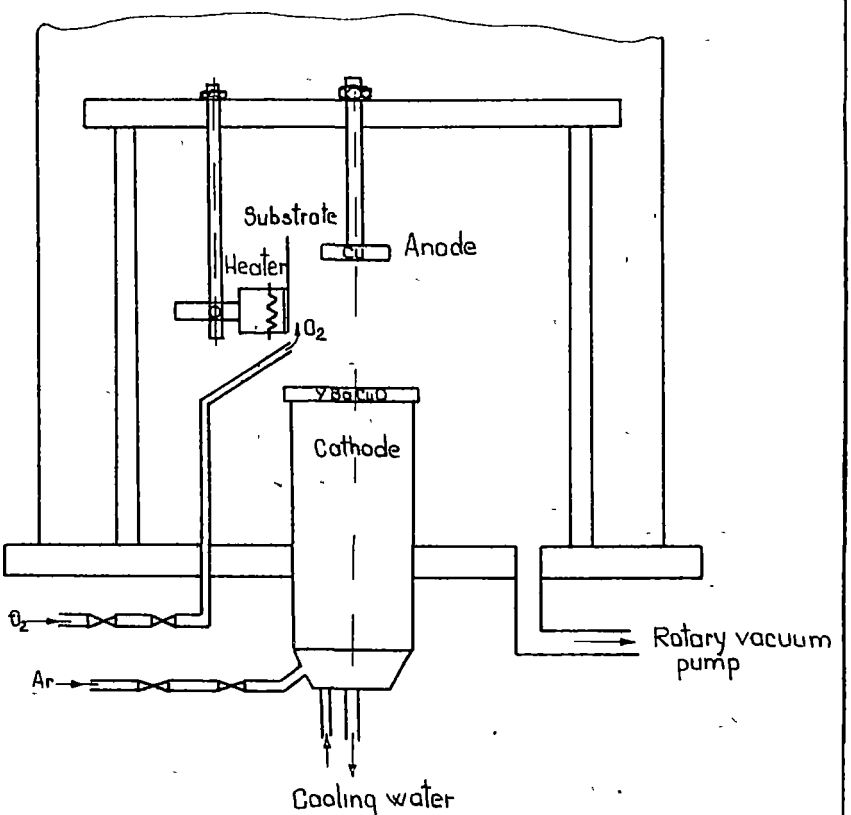

Fig 3. THE OFF-AXIS GEOMETRY

REFERENCES

1. Hebard A.F.,Eick R.H., Fiory A.F., and Short K.T., Proceedings of the Forth Annual 1988 Northest Regional Meeting "Processing and Applications of High-Tc Superconductors".
2. Kellett B.J., James J.H., Gauzzi A., Dwir B., Affronte M., and Pavuna D., Proc. of the Material Research Society 169, 1990, 639.
3. Fork D.K., Geballe T.H., Boyce J.B., Ponce F.A., Johnson R.I., IEEE Transactions on Magnetics, 25, 2, 1989, 2426.
4. Dijkkamp D., Venkatesan T., Wu X.D., Shaheen S.A., Jisrawi N., Min-Lee Y.H., McLean W.L., and Croft M., Appl.Phys.Lett. 51, 8, 1987, 619.
5. Habermeier H.U., WAgner G., and Mertens G., preprint.
6. Tomlinson E.J., BArber Z.H., Morris G.W., Somekh R.E., and Evetts J.E., IEEE Transactions on Magnetics 25, 2, 1989, 2530.
7. Hong M., Liou S.H., Kwo J., and Davidson B.A., Appl.Phys.Lett.51, 9, 1987, 694.
8. Poppe U., Schubert J., Arons R.R., Evers W., Freiburg C.H., Reichert W., Schmidt K., Sybertz I., and Urban K., Solid State Communications 66, 6, 1988, 661.
9. Xi X.X., Linker G., Meyer O., Nold E., Obst B., Ratzel F., Smithey R., Strehlan B., Weschenfleder F., and Geerk J., Z. Phys. B-Condensed Matter 74, 1989, 13.
10. Mantese J.V., Hamdi A.H., Micheli A.L., Chen Y.L., Wong C.A., Johnson J.L., Karmarker M.M., and Padmanabhan K.R., Appl.Phys.Leet. 52, 19, 1988, 1631.
11. Nasu H., Makida S., Kato T., Ibahara Y., Imura T., and Osaka I., Chemistry Lett. 1987, 2403.
12. Norris P.E., Orlando G.W., Superconductor Industry, spring 1990, 14.
13. Yamane H., Kurosawa H., and Hirai T., Proc. 7-th European Conf. on CVD, Perpignon, France, 19-23 June 1989.
14. Tabuchi J. and Utsumi K., Appl. Phys. Lett. 53, 17, 1988.
15. Yoshihara K., Kagata K., Yokoyama S., Hiroki T., Higuma H., Yamazaki T., and Nakahigashi K., Japanese Journal of Applied Phys. 27, 8, 1988, L 1492.
16. Campuno L.A., Newman N., Superconductor Industry, spring, 1990, 34.
17. Stark F., Z. Electrochem. 15, 1909, 509.

FIGURE CAPTION

1. Cross-section of the cathode magnetron gun.
2. Heating-holding system.
3. Off-axis sputtering geometry.

În cel de al XXXVII-lea an (1992) *Studia Universitatis Babeş-Bolyai* apare în următoarele serii:

matematică (trimestrial)
fizică (semestrial)
chimie (semestrial)
geologie (semestrial)
geografie (semestrial)
biologie (semestrial)
filosofie (semestrial)
sociologie-politologie (semestrial)
psihologie-pedagogie (semestrial)
ştiinţe economice (semestrial)
ştiinţe juridice (semestrial)
istorie (semestrial)
filologie (trimestrial)

In the XXXVII-th year of its publication (1992) *Studia Universitatis Babeş-Bolyai* is issued in the following series:

mathematics (quarterly)
physics (semesterily)
chemistry (semesterily)
geology (semesterily)
geography (semesterily)
biology (semesterily)
philosophy (semesterily)
sociology-politology (semesterily)
psychology-pedagogy (semesterily)
economic sciences (semesterily)
juridical sciences (semesterily)
history (semesterily)
philology (quarterly)

Dans sa XXXVII-e année (1992) *Studia Universitatis Babeş-Bolyai* paraît dans les séries suivantes:

mathématiques (trimestriellement)
physique (semestriellement)
chimie (semestriellement)
geologie (semestriellement)
géographie (semestriellement)
biologie (semestriellement)
philosophie (semestriellement)
sociologie-politologie (semestriellement)
psychologie-pédagogie (semestriellement)
sciences économiques (semestriellement)
sciences juridiques (semestriellement)
histoire (semestriellement)
philologie (trimestriellement)